Genetic factors affecting immune phenotypes in type 1 diabetes

Xiaojing Chu[1,2,3,+], Anna W.M. Janssen[4,+], Hans Koenen[5,+], Linzhung Chang[1], Xuehui He[5], Irma Joosten[5], Rinke Stienstra[4,6] Yunus Kuijpers[2,3], Cisca Wijmenga[1], Cheng-Jian Xu[2,3,4], Mihai Netea[4,7], Cees J. Tack[*4], Yang Li[*1,2,3,4]

Affiliations:

[1.] Department of Genetics, University of Groningen, University Medical Center Groningen

[2.] Centre for Individualised Infection Medicine, CiiM, a joint venture between the Hannover Medical School and the Helmholtz Centre for Infection Research, Hannover, Germany

[3.] TWINCORE, Centre for Experimental and Clinical Infection Research, a joint venture between the Hannover Medical School and the Helmholtz Centre for Infection Research, Hannover, Germany

[4.] Department of Internal Medicine, Radboud University Medical Center, Nijmegen, the Netherlands.

[5.] Department of Laboratory Medicine, Laboratory Medical Immunology, Radboud University Medical Center, Nijmegen, the Netherlands.

[6.] Division of Human Nutrition and Health, Wageningen University, the Netherlands.

[7.] Department for Genomics & Immunoregulation, Life and Medical Sciences Institute (LIMES), University of Bonn, Bonn, Germany.

[+] **Shared first authors**
*** Shared last and corresponding authors**
Yang Li
Yang.Li@helmholtz-hzi.de
Cees J. Tack
Cees.Tack@radboudumc.nl

Abstract:

Large inter-individual variability in immunological cell composition and function determines immune responses in general and susceptibility to immune-mediated diseases in particular.

While much has been learned about the genetic variants relevant for type 1 diabetes, the pathophysiological mechanisms through which these variations exert their effects are unknown. In this study, we characterize the genetic factors influencing immune responses in patients with type 1 diabetes. Genetic variants that determine susceptibility to T1D significantly affect T cell composition. Specifically, the CCR5+ regulatory T cells associate with T1D through the CCR region, suggesting a shared genetic regulation. Genome-wide quantitative trait loci (QTL) mapping analysis of immune traits revealed 15 genetic loci that influence immune responses in T1D. Among them, 12 have never been reported in healthy population studies, implying a disease-specific genetic regulation. Altogether this study provides new insights into the genetic factors that affect immunological responses in T1D.

Key words: functional genomics, type 1 diabetes, immune function

45

46 **Introduction**

47 T1D is a common, chronic, autoimmune disease, characterized by destruction of insulin-
48 producing beta-cells in the pancreas that results in lifelong dependence on exogenous insulin and
49 is associated with a high morbidity and mortality *(Atkinson et al., 2014)*. The causes and
50 immunological pathways responsible for the development of T1D are still incompletely
51 understood, which hampers the efforts to identify an etiopathogenetic treatment.

52 Many studies have highlighted the role of environmental, genetical, and immunological factors
53 in the pathogenesis of T1D*(Pociot and Lernmark, 2016; Rewers and Ludvigsson, 2016)*.
54 Environmental factors such as overweight, infections, microbiome composition and dietary
55 deficiencies have been reported as risk factors for T1D*(Rewers and Ludvigsson, 2016)*. In turn,
56 the immunological pathogenesis*(Cabrera et al., 2016)* of T1D includes innate inflammation and
57 adaptive immunity, such as enhanced T cell responses*(Hundhausen et al., 2016)*. Large genome-
58 wide association studies (GWAS) performed in the last two decades have underscored the
59 contribution of genetic polymorphisms for the susceptibility to T1D: ~60 genomic loci
60 associated with T1D risk have been identified (Barrett et al., 2009; Bradfield et al., 2011; Cooper
61 et al., 2008; Grant et al., 2009; Huang et al., 2012; Onengut-Gumuscu et al., 2015; Ram et al.,
62 2016). While these loci show significant enrichment in specific immune-related biological
63 pathways such as cytokine signaling and T cell activation*(Barrett et al., 2009; Cooper et al.,*
64 *2008)*, the functional consequences of many of these loci and genetic variants are still unknown.
65 We thus lack the information that could link the genetic susceptibility factors to the
66 immunological pathways potentially important for T1D pathogenesis. The genetically-regulated

67 inflammatory response signature in T1D may also be relevant for the inflammatory response in
68 general and may become modified by the chronic hyperglycemic state.

69 In the present study we aimed to comprehensively describe the immunopathological
70 consequences of the genetic variants linked to T1D susceptibility, using a high-throughput
71 functional genomics approach. As a part of the Human Functional Genomics Project
72 (HFGP)*(Netea et al., 2016)*, we carried out deep immunophenotyping in peripheral blood
73 samples from a cohort of 243 T1D patients (300DM), covering cell subpopulation composition
74 and cytokine production upon stimulations, as proxies of immunological function. Part of the
75 results were compared to those obtained in a population-based cohort of 500 healthy individuals
76 (500FG), that successfully characterized the impact of genetic factors *(Aguirre-Gamboa et al.,*
77 *2016; Li et al., 2016)* on immune responses in healthy individuals. Here, we systematically
78 evaluate the genetic regulation on the immune phenotypes in T1D, and show how genetic
79 variation affects immune cell traits and cytokine production in response to stimulations. In total,
80 we identified 15 genome wide significant genomic loci (P value $< 5 \times 10^{-8}$) associated with
81 immune phenotypes in the 300DM cohort. Among them, 12 loci have never been reported in any
82 healthy population study. These data provide a deeper understanding of the immune mechanisms
83 involved in the pathophysiology of T1D and affecting the general inflammatory response and
84 may open avenues towards the development of novel diagnostics and potentially
85 immunotherapies.

86

87 **Results**

88 *Interrelationship between immune cell counts and cytokine production in T1D.*

89 We collected blood samples from 243 T1D patients (300DM cohort, Figure 1—figure
90 supplement 1), following the same methodology as previously described (Aguirre-Gamboa et al.,
91 2016; ter Horst et al., 2016; Li et al., 2016). The baseline characteristics of the 300DM and a
92 cohort of healthy individuals (500FG) are shown in Supplementary file 1. Their median age was
93 53.5 years (range 20-85), and they had a median diabetes duration of 28 years (range 1-71 yrs).
94 Hence, the cohort generally consisted of middle-aged people with long standing type 1 diabetes.
95 We measured 72 types of immune cells covering both lymphocytes and monocyte lineages and
96 10/6 (300DM/500FG) different cytokines released in response to stimulation with four types of
97 human pathogens in both cohorts (Figure 1A, Figure 1—figure supplement 2).
98 The nonmetric multidimensional scaling plot illustrates the interrelationship among immune
99 cells' abundance (Figure 1B), and cytokine production levels (Figure 1C) in T1D patients. We
100 observed a separation of the B cell subpopulations cluster from the T cell, monocyte, and NK
101 cell population clusters. This observation suggests that T cells, monocytes, and NK cells have
102 more interplay than B cells at baseline, which is consistent with our previous finding in a healthy
103 cohort (500FG(Aguirre-Gamboa et al., 2016)). Furthermore, cytokine features are clustered
104 based on their cellular origins, with a partially overlapping cluster between monocyte-derived
105 cytokines and T cell-derived cytokines, Figure 1C). This may suggest activation of a co-
106 regulatory network of monocyte-derived and T cell-derived cytokine production capacity in
107 T1D.
108 To obtain a comprehensive interaction map between immune cells and cytokines, we correlated
109 each of the immune cell counts with each of the cytokine production profiles (IL-1β, IL-6, TNF-
110 α, IL-10, IL-1RA, IL-8, MCP-1, IFNγ, IL-17, and IL-22) in response to 21 stimulations.
111 Cytokine levels were hierarchically clustered based on correlation coefficients with immune cell

112 counts (Figure 1D). In line with the functional relationship between immune cells and cytokines,
113 we observed positive correlations between monocyte lineages and monocyte-derived cytokines
114 (IL-1β, IL-6, TNF-α, IL-10, IL-1RA, IL-8, and MCP-1), as well as between T cell subsets and T
115 cell-derived cytokines (IFNy, IL-17, and IL-22) (indicated by red color in Figure 1D). Besides,
116 we found a negative correlation between monocyte-derived cytokines production in response to
117 four distinct types of stimulations (bacteria, fungi, non-microbial and TLR ligands) and
118 lymphocyte counts (blue, Figure 1D). We observed similar correlation patterns in 500FG (Figure
119 1—figure supplement 3). This correlation matches the findings that a high abundance at baseline
120 of adaptive immune cells is associated with a lower production of monocytes derived cytokines
121 after stimulation*(Dong Kim et al., 2007)*, which is not altered by T1D status. Overall, the inter-
122 relationships between immune cells and cytokines in response to stimulations are rather similar
123 in T1D as compared to healthy individuals.

124

125 *Impact of T1D GWAS SNPs on immune phenotypes in T1D patients*

126 Considering that T1D is a multifactorial disease with a genetic component, we tested whether the
127 known risk variants of T1D affect immune phenotypes and function. We firstly checked SNPs
128 within HLA locus in our association studies on cell proportion and cytokine production level.
129 Consistent with our previous findings in 500FG, we did not observe any significant associations
130 of HLA allelic variants in 300DM.

131 Non-HLA genetic loci from published GWAS studies of European background were acquired
132 from the GWAS-catalog (Nov 2019)*(Buniello et al., 2019).* Among them, genetic variants in 63
133 independent T1D loci were present in our data, and we found that 13 out of these 63, indeed

134 associated with susceptibility to T1D with nominal significance (P value < 0.05) (Supplementary
135 file 2).

136 Next, we investigated whether these genetic risk loci for T1D affect immune parameters and
137 function. The quantile-quantile (Q-Q) plot of the association of the 63 T1D GWAS loci with
138 different cell types and cytokines illustrates an inflated deviation from an expected uniform
139 distribution (Figure 2A, Figure 2—figure supplement 1). We further tested whether this
140 deviation can be explained by chance by comparing the association of immune traits with T1D
141 GWAS SNPs with that of 1000 randomly selected independent SNPs (Figure 2B, Methods). The
142 p value shows that the T1D GWAS SNPs are enriched in association with T-cell traits in the
143 T1D cohort (P value = 0.007).

144 A pair-wise association analysis between T1D GWAS loci and immune phenotypes shows that
145 261 out of 269 immune cell phenotypes and 53 out of 55 cytokine-stimulation pairs are
146 suggestively associated with at least one T1D GWAS locus (P value < 0.05, Supplementary files
147 3, 4). We further applied a permutation-based approach to test whether immune phenotypes were
148 significantly influenced by the accumulative effects of these 63 GWAS loci (Methods).
149 Compared to random sets of independent SNPs, the 63 T1D GWAS loci explain significantly
150 more variance of 27 cell sub proportions and 15 cytokine production traits (P value < 0.05,
151 Figure 2C, Figure 2—figure supplement 2A, B). As shown in the heatmap (Figure 2C,
152 arrowhead), a T1D risk allele rs11574435-T, in strong LD (r^2 = 0.95) with the T1D GWAS SNP
153 rs113010081*(Onengut-Gumuscu et al., 2015)*, is associated with higher percentage of many
154 CCR5+ CD4+ T-cell traits and lower percentage of CCR5- CD4+ T-cell traits. Chemokine
155 signaling pathways regulate the migration of cells from the circulation (PBMCs) to the tissue
156 (pancreases).

157 To further validate the importance of chemokine signaling mediated by *CCR5* in T1D, we
158 illustrated the transcriptional changes on *CCR5* and its corresponding ligand genes using publicly
159 available data from transcriptome analysis in PBMCs and pancreatic tissue from T1D patients
160 and controls *(Planas et al., 2010; Yang et al., 2015)*(See also Methods), and found significant
161 expression changes of *CCR5*, *CCL5*, and *CCL4* in T1D patients, suggesting the involvement of
162 this chemokine ligand - chemokine receptor pathway (Figure 3A). Besides, another top SNP-
163 rs35092096 within the *CCR* genes region has the strongest effects on many CCR5 Tregs
164 proportions in T1D. For example, the minor allele T in rs35092096 associates with a higher ratio
165 of CCR6+CCR7-CCR5+ Tregs/ CCR6+ T regs (Figure 3B, C). Together with the observed
166 regulation from a GWAS locus within the *CCR* region on CCR6+CCR7-CCR5+ Tregs
167 proportion, we tested whether CCR6+CCR7-CCR5+ Tregs and T1D shared the same causal
168 variants/genomic regions by integrating the cell proportion QTL of CCR6+CCR7-CCR5+ Tregs
169 and the latest T1D GWAS profile using colocalization analysis*(Giambartolomei et al., 2014)*.
170 The result strongly supports that CCR6+CCR7-CCR5+ Tregs share the same regulatory genomic
171 region with T1D, although the causal SNP might be different (Figure 3D, H3 = 0.95).
172 Altogether, these results support a role of the *CCR* region on Tregs function in the pathogenesis
173 of T1D.

174 Overall, we observed that T1D GWAS loci influence immune cell proportion and cytokine
175 production capacity, again stressing the importance of T cell immunity in the genetic regulation
176 of T1D.

177

178 *Genetic regulation of immune phenotypes in T1D*

179 To further explore potential genetic regulation of immune phenotypes on the whole-genome
180 level, we performed quantitative trait loci (QTL) mapping in 300DM. We identified nine
181 genome-wide significant QTLs (P value < $5x10^{-8}$) associated with immune cell proportion,
182 including four associated with T cell subpopulations expressing specific chemokine receptors
183 (e.g., rs35092096 and rs7614884) (Figure 4A, top and middle panels, Supplementary file 5). A
184 pathway analysis of the cell proportion QTLs shows significant enrichment in chemokine and
185 cytokine signaling-related biological pathways (FDR < 0.05, Figure 4—figure supplement 1A),
186 highlighting the effects of immune signaling genes in cell proportion regulation.
187
188 In parallel, we detected six significant genomic loci associated with cytokine production in
189 response to stimulations by QTL mapping in 300DM (Figure 4A, bottom panel, Supplementary
190 file 5). TLR-related pathways significantly enrich cytokine production QTLs (FDR < 0.05,
191 Figure 4—figure supplement 1B). A missense variant, rs5743618, on the *TLR1* gene, affects IL-6
192 production in response to *S.pneumoniae* in PBMC. Previously, we observed the strong effect of
193 the TLR locus on cytokine levels in controls*(Li et al., 2016)*. Our results support the reported
194 function of TLRs in detecting pathogens (including bacterial) and triggering the release of
195 inflammatory cytokines*(Fitzgerald and Kagan, 2020)*.
196
197 Next, to identify the consistent immune phenotype QTLs within T1D patients and healthy
198 individuals, and to expand our understanding on genetic regulation of immune phenotypes, we
199 applied a meta-analysis by integrating the obtained QTLs from the 300DM and 500FG cohorts.
200 In total, we newly identified ten genetic loci that were associated with immune cell proportion
201 (Figure 4A, top panel, colored in red) and three genetic loci that were associated with cytokine

202 production (Figure 4A, bottom panel, colored in red), including a *CD5* locus significantly
203 associated with IgD+ CD5++ proportion in B cells (Supplementary file 5). This may be
204 important as recent studies report the relevance of IgD+ CD5++ B cells in T1D*(Saxena et al., 2017)* as well as within other autoimmune diseases such as Graves' disease*(van der Weerd et al., 2013)*.
207
208 To summarize, we identified 28 genetic loci associated with either immune cell traits or cytokine
209 production phenotypes. Among them, the genes within 11 loci (+- 250kb window) are druggable
210 according to public drug database*(Finan et al., 2017)*, including *COL13A1*, *CCR* family genes,
211 *ROR2*, *NOS1*, *IL-10*, *IL-6*, *STK33*, *NELL1*, *FCGR2A*, *CD5* and *TLR1* (Supplementary file 5).
212 Some of these genes are already therapeutic targets in other autoimmune diseases, such as the
213 *STK33* inhibitor for rheumatoid arthritis treatment*(Rolf et al., 2015)*.
214 It is also worth mentioning that, as far as we know, 12 out of the 28 significant loci have never
215 been reported in other healthy individual population cohorts according to records in
216 PhenoScanner V2 (Kamat et al., 2019) (P value $< 1 \times 10^{-5}$, November, 2019), neither were they
217 identified in the 500FG cohort (P value < 0.05). An example of a T1D specific locus is that
218 rs4744112 located on chromosome 9 has an influence on CCR6+CXCR3+CCR4- Th1 like
219 helper proportion (Figure 4B), with minor allele G leading to a decrease in these cells relative to
220 major allele T (Figure 4C). rs4744112 is located within the transcriptional starting site (TSS) and
221 enhancer regions*(Roadmap Epigenomics Consortium et al., 2015)* of *ROR2*.
222
223 *Functional Clues from the Associated Variants in T1D patients*

224 In order to understand the mechanism behind the genetic regulations of immune response in
225 T1D, we next explored the function of identified genetic factors of immune phenotypes. We
226 noticed that SNPs within the 28 immune parameter QTLs are mostly located in the intergenic
227 and intronic region (Figure 4—figure supplement 2), suggesting that identified genetic variants
228 influence immune phenotypes through regulatory effects rather than through protein structure
229 alteration. Moreover, seven out of 28 loci influence blood gene expression in public
230 databases*(Carithers and Moore, 2015; Westra et al., 2013)* (Supplementary file 5) including
231 rs7512140: FCGR2B/FCRLB, rs35092096: CCR1/CCR3, rs4744112: ROR2/SPTLC1,
232 rs10840031: TRIM66, rs800139: C11orf21, rs1518110: IL10 and rs56350303: AC091814.2.
233 These indicate the potential functional genes behind the identified genetic loci.
234
235

236 **Discussion**

237 The present study applies a high-throughput functional genomics approach to identify the
238 association between genetic factors and the inflammatory phenotype in patients with T1D. The
239 results confirm a correlation between baseline immune cell populations and ex vivo cytokine
240 production in response to bacteria, fungi, non-microbial and TLR ligand stimulations. We
241 provide evidence for a direct link between T1D GWAS loci and immune functionality,
242 particularly on circulating T cell subpopulations. We show that T cell alteration is largely driven
243 by T1D genetics, while B cells do not show a significant association with T1D GWAS loci. The
244 association between the proportion of CCR5+ Tregs and T1D susceptibility through CCR genes
245 suggests that T1D associated genetic variants contribute to immune function alteration through
246 an accumulative effect. Finally, out of 28 genome-wide significant genetic loci regulating

247 immune cell proportions and cytokine production, we identified 12 immune phenotype QTLs
248 specific to 300DM. We also found 11 druggable genes as candidates for therapeutic intervention.
249 Altogether, this study provides several novel insights into the genetic variability of immune traits
250 in T1D.

251 Our finding of a correlation between baseline immune cells and cytokine production in response
252 to bacteria, fungi, non-microbial and TLR ligand stimulations, suggests that steady-state immune
253 cell abundance and alteration of immune cell proportion also affects immune response. This is in
254 line with earlier findings on the regulation between immune cells and cytokine production*(Dong*
255 *Kim et al., 2007)*. This finding has two important consequences: the immune response variability
256 could be partly explained by variation in steady-state, and treatment of steady-state immune cells
257 before stimulation could also influence immune response after stimulation.

258 Studies comparing T1D patients and healthy controls show that immune-related genes are
259 physically located in T1D loci or differentially expressed. More studies highlight the importance
260 of T cell immunity in T1D pathology*(Farh et al., 2015)*. In our study, we provide evidence for a
261 direct link between T1D GWAS loci to immune functionality, particularly on circulating T cell
262 subpopulations. We show that T cell alteration is largely genetically driven, while, interestingly,
263 B cells do not show a significant association with T1D GWAS loci. It is thus tempting to
264 speculate that the occurrence of auto-antibodies in T1D patients have limited pathophysiological
265 relevance, but are merely markers of an autoimmune process mainly driven by T-cells as
266 suggested before (Martin et al., 2001).

267

268 Importantly, we reveal that the effects of different GWAS loci on immune phenotypes vary.
269 Despite the strong effects of the CCR locus (mean absolute effect sizes = 0.017 (cell proportion),

270 0.15 (cytokine production)), we observed much weaker individual effects from other T1D
271 GWAS loci on immune cell proportion parameters (mean absolute effect size = 0.0060) and/or
272 cytokine production (mean absolute effect size = 0.10) (Figure 2C and Figure 2—figure
273 supplement 2). This finding indicates that T1D-associated genetic variants might alter immune
274 function through a cumulative effect. Considering the complexity of the immune system, it may
275 be an alternative explanation for our finding that T1D associated genetic variants that affect
276 immune functions differ from genetic variants that affect immune cell proportion and cytokine
277 production capacity.
278
279 Despite the limited sample size, we identified 28 genome-wide significant genetic loci regulating
280 immune cell proportions and cytokine production in T1D patients and health. Among them, 12
281 immune phenotype QTLs are specifically found in 300DM, but not in healthy volunteers,
282 suggesting a distinct regulatory mechanism of immune parameters and functions between disease
283 and health. More importantly, in our study, we highlight 11 druggable genes as candidates for
284 therapeutic intervention.
285 The data presented in our study are generated from PBMC. While these likely reflect overall
286 immune function, some immune cell types may not be captured and all over the findings refer to
287 changes in circulating factors that may not necessarily reflect changes occurring in relevant
288 immune organs, such as pancreatic islets, gut or lymph nodes. Still, islet infiltrating immune cells
289 do originate from circulating blood cells, and circulating chemokines/cytokines are important in
290 activating and recruiting immune cells. Hence, the circulating level of immune cells and cytokine
291 production capacity is probably relevant for local tissue immunity.

292 We acknowledge that our study has limitations. Firstly, 300DM and 500FG were recruited and
293 measured at two years apart, although established using an identical setting, the same protocol
294 and in the same lab. There may thus be some differences in the absolute immune cell counts or
295 cytokine levels due to a batch effect. Therefore, this study was not designed as a case-control
296 study, but the healthy controls were used to compare genetic associations identified in the T1D
297 cohort. Secondly, young people were overrepresented in 500FG. Although age has been
298 regressed out in both of the cohorts, there might be a bias in the genetic mapping. Finally, our
299 type 1 diabetes-specific analyses should be viewed exploratory as they have not been validated in
300 a separate cohort. Our study has also strengths: it applied cutting-edge technologies to assess
301 immune cell function and genetic variation, and it is the first study which comprehensively
302 combines 'omics' technologies to abundant phenotyping in a rather large group of participants to
303 explain between individuals' variation in immune responses.
304

305 **Conclusions**

306 In conclusion, we applied a novel high-throughput functional genomics approach, and show that
307 genetic factors regulate immune responses in T1D patients. We show genetic susceptibility to
308 immune phenotypes in patients with T1D, and highlight the importance of T cell immunity in the
309 genetic regulation of T1D. We identify specific cell populations that are likely involved in
310 pathophysiology of T1D (CCR5+ T-regs). Together, these findings may provide an avenue
311 towards identification of novel preventive and therapeutic treatments.
312

313 **Materials and Methods**

314 **Study cohort.** This study mainly focuses on a 300DM cohort, and involves a 500FG cohort (part
315 of HFGP*(Netea et al., 2016)*). In total, 132 males and 111 females of Caucasian origin with T1D
316 were recruited in the 300DM cohort at the Radboudumc, the Netherlands. Their age ranges from
317 20 to 84 years. Detailed information of 500FG cohort can be found in the previous
318 publications(Aguirre-Gamboa et al., 2016; ter Horst et al., 2016; Li et al., 2016).
319
320 **Measurement of Immune Cell composition.** Myeloid and lymphoid immune cell levels were
321 measured by 10-color flow cytometry. The parental and grandparental proportion from 73
322 manually annotated immune cells as well as the proportion of CD4+ T cells, CD8+ T cells,
323 memory T regulatory cells and monocytes carrying chemokine receptors: CCR6 (CD196),
324 CXCR3 (CD183), CCR4 (CD194), CCR5 (CD195) and CCR7 (CD197) were calculated
325 respectively, and end up with 269 immune cell traits of the 300DM cohort. We used the same
326 gating strategy of measuring cell subpopulations as 500FG (See reference*(Aguirre-Gamboa et*
327 *al., 2016)* and Figure 1—figure supplement 2).
328
329 **Stimulation of PBMCs and measurement of Cytokine production capacity.** Isolation of
330 PBMCs were washed twice with cold phosphate-buffered saline (PBS) and suspended in Roswell
331 Park Memorial Institute (RPMI) 1640 Dutch-modified culture medium (Gibco/Invitrogen, Breda,
332 the Netherlands) supplemented with 50 mg/l gentamycin (Centraform), 1 mM pyruvate
333 (Gibco/Invitrogen) and 2mM L-glutamine (Gibco/Invitrogen). Cells were counted on a Sysmex
334 XN-450 Hematology Analyzer (Sysmex Corporation, Kobe, Japan).
335 For *in vitro* stimulation experiments, $5x10^5$ cells/well were cultured for 24hr or 7 days at 37°C
336 and 5% CO_2 in 96-well round-bottom plates (Greiner). For the 7 days' cultures, medium was

337 supplemented with human pooled serum (pooled from healthy blood donors, end concentration
338 10%). Supernatants were collected and stored in -20°C until used for ELISA.
339 The following stimulations were used: (LPS (100ng/ml, 1ng/ml), Pam3cys, *Borrelia* mix, *C*.
340 *albicans* conidia, *C*. *albicans* hyphae, Imiquimod (IMQ), *S*. *aureus*, *S*. *pneumoniae*, palmitic acid
341 (C16), C16+ monosodium urate crystals (MSU), *E*. *coli*, *M*. *tuberculosis* (MTB), *B*. *burgdorferi*,
342 *C*. *burnetii*, *C*. *neoformans*, Oxidized low-density lipoprotein (OxLDL), OxLDL+ LPS,
343 Polyinosinic:polycytidylic acid (Poly IC), *Rhizopus* microspores, *Rhizopusoryzae*)*(Li et al*.,
344 *2016)*. Concentrations of monocyte-derived cytokines (IL-1β, IL-6, TNF-α, IL-8, IL-10, IL-1Ra,
345 MCP-1) and T cell-derived cytokines (INF-γ, IL-17, IL-22) in response to various stimulations
346 were measured in peripheral blood mononuclear cells (PBMC) by ELISA kits following the
347 manufacturers protocol. For all cytokines commercially available kits were used (R&D Systems,
348 MN, USA or Sanquin, Amsterdam, the Netherlands).
349
350 **Genotyping, quality control and imputation.** DNA samples of 224 Dutch T1D patients were
351 collected and genotyped by the Infinium® Global Screening Array. The genotype calling was
352 performed using Opticall 0.7.0*(Shah et al*., *2012)* with default settings (call rate > 0.99). Two
353 samples were removed due to contamination or mislabeling; one sample from a related
354 individual (identity be descent > 0.185) was removed and six genetic outliers were identified by
355 either heterozygosity rate check (individuals with heterozygosity rate heterozygosity rate ± 3
356 standard deviations from the mean were excluded) or multi-dimensional scaling (MDS) plots of
357 samples merging with 1000 Genomes data, leaving 215 samples, which show good consistence
358 with European samples from 1000 Genomes data (Figure 1—figure supplement 1) according to
359 standard protocol (Anderson et al., 2010). DNA samples from the 500FG cohort were genotyped

360 by Illumina Human OmniExpress Exome-8 v1.0 SNP chip. Outliers were excluded according to
361 population relationship, medication and disease information. Details can be found in our
362 previous studies in 500FG*(Aguirre-Gamboa et al., 2016; Li et al., 2016)*. Single-nucleotide
363 polymorphisms (SNPs) with a minor allele frequency (MAF) < 0.001 were removed from each
364 cohort, and a Hardy-Weinburg equilibrium (HWE) P value < 1×10^{-5} were removed for the
365 healthy cohort (500FG). By taking shared genetic variants, we merged the 300DM cohort and
366 500FG cohort, and we used an online genotype imputation service provided by Michigan
367 Imputation Server (https://imputationserver.sph.umich.edu)*(Das et al., 2016)* with HRC Panel
368 1.1 as reference. SNPs with low imputation quality (R2 < 0.3) and/or MAF < 0.01 in all imputed
369 samples and/or HWE p values < 1×10^{-5} in healthy individuals were excluded leaving 4304387
370 SNPs and 666 individuals (N_{300DM} = 215 and N_{500FG} = 451).
371
372 **Preprocess of the data**
373 Immune cell proportion was calculated by dividing counts of their parental and grandparental
374 cell types (Supplementary file 6). An inverse rank transformation(Aguirre-Gamboa et al., 2016;
375 Orrù et al., 2013) was applied on the proportion values for genetic association analysis. Cytokine
376 levels were log2 transformed.
377
378 **Immune parameter QTL mapping.** After intersecting with available genotype data and
379 excluding volunteers with a mixture or another genetic background, 214 were left for immune
380 parameter quantitative trait locus (QTL) mapping. We next evaluated covariates influencing
381 immune function. Associations with age, gender, seasonal effects were calculated using
382 previously described methods(Aguirre-Gamboa et al., 2016; ter Horst et al., 2016; Li et al.,

383 2016), i.e. Spearman correlation analysis and linear regression model. Significance was declared
384 after multiple testing correction (FDR < 0.05). Age significantly associated with 129/269
385 immune cell traits and 12/55 cytokine traits; gender associated with 59/269 immune cell traits
386 and 5/55 cytokine traits; seasonal effects associated with 121/269 immune cell traits and 38/55
387 cytokine traits (Figure 4—figure supplement 3). Thus, we took age, gender and seasonal effects
388 as covariates in the linear regression for both immune cell proportion QTL mapping as well as
389 cytokine QTL mapping. Besides, considering the effect of immune cell proportion on cytokine
390 production, we took major cell types, including monocyte, lymphocyte, T cell, B cell and NK
391 cell proportion in PBMC as covariates in a linear model for cytokine QTL mapping, as we
392 previously did*(Li et al., 2016)*. Linear regression function was applied with an R package
393 Matrix-eQTL*(Shabalin, 2012)* for immune parameter QTL mapping, and software
394 METAL*(Willer et al., 2010)* was applied to summary statistics from both cohorts for meta-
395 analysis, in which the model based on effect size and standard error with default settings were
396 used. P values < 5×10^{-8} were considered to be genome-wide significant. Lambda values were
397 calculated indicating no obvious inflations (0.977-1.026).
398
399 **Extraction of T1D GWAS SNP list.** We downloaded a summary of T1D GWAS results from
400 GWAS-catalog (https://www.ebi.ac.uk/gwas/)*(Buniello et al., 2019)* in November 2019, and
401 removed studies done in non-European-ancestry populations. Top SNPs within LD ($r^2 > 0.1$)
402 from different studies were considered as the same locus, and SNPs with the lowest p value were
403 taken into analysis. We noticed that the effect directions of some SNPs were unclear or
404 inconsistent in different studies. In this case, we assigned directions according to the newest
405 GWAS study*(Onengut-Gumuscu et al., 2015)*.

406

407 **GWAS analysis of 300DM cohort for the known T1D loci.** We extracted all proxies in strong
408 LD with top SNPs from published T1D GWAS (Case-Control) studies ($r^2 > 0.8$) and performed a
409 chi-square test on clinical status by using PLINK 1.9. Samples in 300DM were taken as cases
410 and samples in 500FG were controls.

411

412 **Impact of T1D GWAS loci on immune phenotypes.** In order to detect the impact of T1D
413 GWAS loci on immune cell populations, we grouped all traits into four categories (B cells, T
414 cells, monocytes and NK cells), and counted the number of suggestive associations (P value <
415 0.05) between 63 top SNPs from T1D GWAS loci and immune cell traits. 1000 permuted sets of
416 63 SNPs were randomly selected from independent SNPs ($r^2 > 0.2$) pruned from all genotyped
417 SNPs. We then compared the associations of the 63 top GWAS SNPs with associations between
418 1000 permutated sets and the same category of immune traits. P value was calculated by the
419 percent of association numbers from permuted sets greater than the association number of the 63
420 T1D GWAS SNPs.
421 We further applied a multivariate linear model to estimate the proportion of variance of each
422 immune phenotype explained by the top SNPs from T1D GWAS loci. We repeated this analysis
423 on 1000 permuted sets of 63 independent SNPs, which were used as reference set. We then
424 compared the null distribution with variance explained by 63 top SNPs from T1D GWAS loci. P
425 value was calculated by the percent of explained variance from permuted sets larger than the
426 variance explained by the 63 T1D GWAS SNPs.

427

428 **Gene expression analysis on *CCR5* and its corresponding ligands genes**. Normalized gene
429 expression data in PBMCs and Pancreases from T1D and controls were acquired from
430 https://www.ebi.ac.uk/gxa*(Papatheodorou et al., 2019)*. A *Student's* t-test was applied to
431 compare gene expression between groups.
432
433 **Post-QTL analysis.** An R package ggplot2 was used to generate Manhattan plots and boxplots.
434 Locus-zoom plots were made by an online tool(http://locuszoom.org)*(Pruim et al., 2010)*. We
435 used an R package coloc*(Giambartolomei et al., 2014)* to perform colocalization analysis with
436 T1D GWAS summary statistics and immune parameter QTLs profile. For pathway analysis**,**
437 genes located within +-10kb of genome wide significant SNPs (p value < 5×10^{-8}) were extracted
438 and analyzed by an online tool FUMA*(Watanabe et al., 2017)* (https://fuma.ctglab.nl).
439 ANNOVAR was used for annotating genetic variants*(Wang et al., 2010)*.
440
441 **Other packages used in this paper.** Pheatmap was used to make heatmaps. Scatter plots and
442 bar plots were generated by ggplot2.
443
444 **References and Notes:**

445 Aguirre-Gamboa, R., Joosten, I., Urbano, P.C.M., van der Molen, R.G., van Rijssen, E., van
446 Cranenbroek, B., Oosting, M., Smeekens, S., Jaeger, M., Zorro, M., et al. (2016). Differential
447 Effects of Environmental and Genetic Factors on T and B Cell Immune Traits. Cell Reports *17*,
448 2474–2487.

449 Anderson, C.A., Pettersson, F.H., Clarke, G.M., Cardon, L.R., Morris, A.P., and Zondervan,
450 K.T. (2010). Data quality control in genetic case-control association studies. Nat Protoc *5*, 1564–
451 1573.

452 Atkinson, M.A., Eisenbarth, G.S., and Michels, A.W. (2014). Type 1 diabetes. The Lancet *383*,
453 69–82.

454 Barrett, J.C., Clayton, D.G., Concannon, P., Akolkar, B., Cooper, J.D., Erlich, H.A., Julier, C.,
455 Morahan, G., Nerup, J., Nierras, C., et al. (2009). Genome-wide association study and meta-
456 analysis find that over 40 loci affect risk of type 1 diabetes. Nat. Genet. *41*, 703–707.

457 Bradfield, J.P., Qu, H.-Q., Wang, K., Zhang, H., Sleiman, P.M., Kim, C.E., Mentch, F.D., Qiu,
458 H., Glessner, J.T., Thomas, K.A., et al. (2011). A genome-wide meta-analysis of six type 1
459 diabetes cohorts identifies multiple associated loci. PLoS Genet. *7*, e1002293.

460 Buniello, A., MacArthur, J.A.L., Cerezo, M., Harris, L.W., Hayhurst, J., Malangone, C.,
461 McMahon, A., Morales, J., Mountjoy, E., Sollis, E., et al. (2019). The NHGRI-EBI GWAS
462 Catalog of published genome-wide association studies, targeted arrays and summary statistics
463 2019. Nucleic Acids Research *47*, D1005–D1012.

464 Cabrera, S.M., Chen, Y.-G., Hagopian, W.A., and Hessner, M.J. (2016). Blood-based signatures
465 in type 1 diabetes. Diabetologia *59*, 414–425.

466 Carithers, L.J., and Moore, H.M. (2015). The Genotype-Tissue Expression (GTEx) Project.
467 Biopreservation and Biobanking *13*, 307–308.

468 Carr, E.J., Dooley, J., Garcia-Perez, J.E., Lagou, V., Lee, J.C., Wouters, C., Meyts, I., Goris, A.,
469 Boeckxstaens, G., Linterman, M.A., et al. (2016). The cellular composition of the human
470 immune system isshaped by age and cohabitation. Nat Immunol *17*, 461–468.

471 Cooper, J.D., Smyth, D.J., Smiles, A.M., Plagnol, V., Walker, N.M., Allen, J.E., Downes, K.,
472 Barrett, J.C., Healy, B.C., Mychaleckyj, J.C., et al. (2008). Meta-analysis of genome-wide
473 association study data identifies additional type 1 diabetes risk loci. Nat. Genet. *40*, 1399–1401.

474 Das, S., Forer, L., Schönherr, S., Sidore, C., Locke, A.E., Kwong, A., Vrieze, S.I., Chew, E.Y.,
475 Levy, S., McGue, M., et al. (2016). Next-generation genotype imputation service and methods.
476 Nat Genet *48*, 1284–1287.

477 Di Benedetto, S., Derhovanessian, E., Steinhagen-Thiessen, E., Goldeck, D., Müller, L., and
478 Pawelec, G. (2015). Impact of age, sex and CMV-infection on peripheral T cell phenotypes:
479 results from the Berlin BASE-II Study. Biogerontology *16*, 631–643.

480 Dong Kim, K., Zhao, J., Auh, S., Yang, X., Du, P., Tang, H., and Fu, Y.-X. (2007). Adaptive
481 immune cells temper initial innate responses. Nat Med *13*, 1248–1252.

482 Dopico, X.C., Evangelou, M., Ferreira, R.C., Guo, H., Pekalski, M.L., Smyth, D.J., Cooper, N.,
483 Burren, O.S., Fulford, A.J., Hennig, B.J., et al. (2015). Widespread seasonal gene expression
484 reveals annual differences in human immunity and physiology. Nat Commun *6*, 7000.

485 Farh, K.K.-H., Marson, A., Zhu, J., Kleinewietfeld, M., Housley, W.J., Beik, S., Shoresh, N.,
486 Whitton, H., Ryan, R.J.H., Shishkin, A.A., et al. (2015). Genetic and epigenetic fine mapping of
487 causal autoimmune disease variants. Nature *518*, 337–343.

488 Finan, C., Gaulton, A., Kruger, F.A., Lumbers, R.T., Shah, T., Engmann, J., Galver, L., Kelley,
489 R., Karlsson, A., Santos, R., et al. (2017). The druggable genome and support for target
490 identification and validation in drug development. Sci. Transl. Med. *9*, eaag1166.

491 Fitzgerald, K.A., and Kagan, J.C. (2020). Toll-like Receptors and the Control of Immunity. Cell
492 *180*, 1044–1066.

493 Giambartolomei, C., Vukcevic, D., Schadt, E.E., Franke, L., Hingorani, A.D., Wallace, C., and
494 Plagnol, V. (2014). Bayesian Test for Colocalisation between Pairs of Genetic Association
495 Studies Using Summary Statistics. PLoS Genet *10*, e1004383.

496 Grant, S.F.A., Qu, H.-Q., Bradfield, J.P., Marchand, L., Kim, C.E., Glessner, J.T., Grabs, R.,
497 Taback, S.P., Frackelton, E.C., Eckert, A.W., et al. (2009). Follow-up analysis of genome-wide
498 association data identifies novel loci for type 1 diabetes. Diabetes *58*, 290–295.

499 ter Horst, R., Jaeger, M., Smeekens, S.P., Oosting, M., Swertz, M.A., Li, Y., Kumar, V.,
500 Diavatopoulos, D.A., Jansen, A.F.M., Lemmers, H., et al. (2016). Host and Environmental
501 Factors Influencing Individual Human Cytokine Responses. Cell *167*, 1111-1124.e13.

502 Huang, J., Ellinghaus, D., Franke, A., Howie, B., and Li, Y. (2012). 1000 Genomes-based
503 imputation identifies novel and refined associations for the Wellcome Trust Case Control
504 Consortium phase 1 Data. Eur. J. Hum. Genet. *20*, 801–805.

505 Hundhausen, C., Roth, A., Whalen, E., Chen, J., Schneider, A., Long, S.A., Wei, S., Rawlings,
506 R., Kinsman, M., Evanko, S.P., et al. (2016). Enhanced T cell responses to IL-6 in type 1
507 diabetes are associated with early clinical disease and increased IL-6 receptor expression. Sci.
508 Transl. Med. *8*, 356ra119-356ra119.

509 Kamat, M.A., Blackshaw, J.A., Young, R., Surendran, P., Burgess, S., Danesh, J., Butterworth,
510 A.S., and Staley, J.R. (2019). PhenoScanner V2: an expanded tool for searching human
511 genotype-phenotype associations. Bioinformatics *35*, 4851–4853.

512 Li, Y., Oosting, M., Smeekens, S.P., Jaeger, M., Aguirre-Gamboa, R., Le, K.T.T., Deelen, P.,
513 Ricaño-Ponce, I., Schoffelen, T., Jansen, A.F.M., et al. (2016). A Functional Genomics
514 Approach to Understand Variation in Cytokine Production in Humans. Cell *167*, 1099-1110.e14.

515 Martin, S., Wolf-Eichbaum, D., Duinkerken, G., Scherbaum, W.A., Kolb, H., Noordzij, J.G., and
516 Roep, B.O. (2001). Development of Type 1 Diabetes despite Severe Hereditary B-Cell
517 Deficiency. N Engl J Med *345*, 1036–1040.

518 Netea, M.G., Joosten, L.A.B., Li, Y., Kumar, V., Oosting, M., Smeekens, S., Jaeger, M., ter
519 Horst, R., Schirmer, M., Vlamakis, H., et al. (2016). Understanding human immune function
520 using the resources from the Human Functional Genomics Project. Nat Med *22*, 831–833.

521 Onengut-Gumuscu, S., Chen, W.-M., Burren, O., Cooper, N.J., Quinlan, A.R., Mychaleckyj,
522 J.C., Farber, E., Bonnie, J.K., Szpak, M., Schofield, E., et al. (2015). Fine mapping of type 1
523 diabetes susceptibility loci and evidence for colocalization of causal variants with lymphoid gene
524 enhancers. Nat. Genet. *47*, 381–386.

525 Orrù, V., Steri, M., Sole, G., Sidore, C., Virdis, F., Dei, M., Lai, S., Zoledziewska, M., Busonero,
526 F., Mulas, A., et al. (2013). Genetic Variants Regulating Immune Cell Levels in Health and
527 Disease. Cell *155*, 242–256.

528 Papatheodorou, I., Moreno, P., Manning, J., Fuentes, A.M.-P., George, N., Fexova, S., Fonseca,
529 N.A., Füllgrabe, A., Green, M., Huang, N., et al. (2019). Expression Atlas update: from tissues to
530 single cells. Nucleic Acids Research gkz947.

531 Planas, R., Carrillo, J., Sanchez, A., Ruiz de Villa, M.C., NuÃ±ez, F., Verdaguer, J., James,
532 R.F.L., Pujol-Borrell, R., and Vives-Pi, M. (2010). Gene expression profiles for the human
533 pancreas and purified islets in Type 1 diabetes: new findings at clinical onset and in long-
534 standing diabetes. Clinical & Experimental Immunology *159*, 23–44.

535 Pociot, F., and Lernmark, Å. (2016). Genetic risk factors for type 1 diabetes. The Lancet *387*,
536 2331–2339.

537 Pruim, R.J., Welch, R.P., Sanna, S., Teslovich, T.M., Chines, P.S., Gliedt, T.P., Boehnke, M.,
538 Abecasis, G.R., and Willer, C.J. (2010). LocusZoom: regional visualization of genome-wide
539 association scan results. Bioinformatics *26*, 2336–2337.

540 Ram, R., Mehta, M., Nguyen, Q.T., Larma, I., Boehm, B.O., Pociot, F., Concannon, P., and
541 Morahan, G. (2016). Systematic Evaluation of Genes and Genetic Variants Associated with Type
542 1 Diabetes Susceptibility. J.I. *196*, 3043–3053.

543 Rewers, M., and Ludvigsson, J. (2016). Environmental risk factors for type 1 diabetes. The
544 Lancet *387*, 2340–2348.

545 Roadmap Epigenomics Consortium, Kundaje, A., Meuleman, W., Ernst, J., Bilenky, M., Yen,
546 A., Heravi-Moussavi, A., Kheradpour, P., Zhang, Z., Wang, J., et al. (2015). Integrative analysis
547 of 111 reference human epigenomes. Nature *518*, 317–330.

548 Rolf, M.G., Curwen, J.O., Veldman-Jones, M., Eberlein, C., Wang, J., Harmer, A., Hellawell,
549 C.J., and Braddock, M. (2015). In vitro pharmacological profiling of R406 identifies molecular
550 targets underlying the clinical effects of fostamatinib. Pharmacol Res Perspect *3*, e00175.

551 Saxena, A., Yagita, H., Donner, T.W., and Hamad, A.R.A. (2017). Expansion of FasL-
552 Expressing CD5+ B Cells in Type 1 Diabetes Patients. Front. Immunol. *8*.

553 Shabalin, A.A. (2012). Matrix eQTL: ultra fast eQTL analysis via large matrix operations.
554 Bioinformatics *28*, 1353–1358.

555 Shah, T.S., Liu, J.Z., Floyd, J.A.B., Morris, J.A., Wirth, N., Barrett, J.C., and Anderson, C.A.
556 (2012). optiCall: a robust genotype-calling algorithm for rare, low-frequency and common
557 variants. Bioinformatics *28*, 1598–1603.

558 Wang, K., Li, M., and Hakonarson, H. (2010). ANNOVAR: functional annotation of genetic
559 variants from high-throughput sequencing data. Nucleic Acids Research *38*, e164–e164.

560 Watanabe, K., Taskesen, E., van Bochoven, A., and Posthuma, D. (2017). Functional mapping
561 and annotation of genetic associations with FUMA. Nat Commun *8*, 1826.

562 van der Weerd, K., Van Hagen, P.M., Schrijver, B., Kwekkeboom, D.J., de Herder, W.W., ten
563 Broek, M.R.J., Postema, P.T.E., van Dongen, J.J.M., Staal, F.J.T., and Dik, W.A. (2013). The
564 peripheral blood compartment in patient with Graves' disease: activated T lymphocytes and
565 increased transitional and pre-naive mature B lymphocytes: T and B lymphocytes in Graves'
566 disease. Clin Exp Immunol n/a-n/a.

567 Westra, H.-J., Peters, M.J., Esko, T., Yaghootkar, H., Schurmann, C., Kettunen, J., Christiansen,
568 M.W., Fairfax, B.P., Schramm, K., Powell, J.E., et al. (2013). Systematic identification of trans
569 eQTLs as putative drivers of known disease associations. Nat Genet *45*, 1238–1243.

570 Willer, C.J., Li, Y., and Abecasis, G.R. (2010). METAL: fast and efficient meta-analysis of
571 genomewide association scans. Bioinformatics *26*, 2190–2191.

572 Yang, M., Ye, L., Wang, B., Gao, J., Liu, R., Hong, J., Wang, W., Gu, W., and Ning, G. (2015).
573 Decreased miR-146 expression in peripheral blood mononuclear cells is correlated with ongoing
574 islet autoimmunity in type 1 diabetes patients. Journal of Diabetes *7*, 158–165.

575

576 **Acknowledgements:**

577 We thank all of the volunteers in the 300DM and 500FG for their participation. We thank Marc
578 J. Bonder for discussions.

579

580 **Funding:**

581 This work was supported by an ERC starting Grant (no. 948207) and a Radboud University
582 Medical Centre Hypatia Grant (2018) to Y.L. and an ERC advanced grant (no. 833247) and a
583 Spinoza grant of the Netherlands Association for Scientific Research to M.G.N. C.T received
584 funding from the Perspectief Biomarker Development Center Research Programme, which is
585 (partly) financed by the Netherlands Organisation for Scientific Research (NWO). AJ was
586 funded by a grant from the European Foundation for the Study of Diabetes (EFSD/AZ
587 Macrovascular Programme 2015). X.C was supported by China Scholarship Council
588 (201706040081).

589

590 **Author contributions:**

591 Y.L., C.T. and M.G.N designed the study. X.C. performed statistical analysis supervised by Y.L.,
592 A.J., H.K., X.H. and I.J. performed the experiments and processed the data. L.C. and C.X. helped
593 with the data analysis. Y.L., C.T., M.G.N, C.W and X.C interpreted the data. Y.L., C.T., M.G.N.
594 and X.C wrote the manuscript with input from all authors.

595

596 **Competing interests:**

597 The authors declare that they have no competing interests.

598

599 **Data and code availability**

600 All raw data of immune phenotypes have been deposited in Dryad
601 (https://doi.org/10.5061/dryad.4f4qrfjd0). Individual genetic data and other privacy-sensitive
602 individual information are available upon request to corresponding authors by email or at Human
603 Functional Genomics Project website (http://hfgp.bbmri.nl). This dataset is not publicly available
604 because it contains information that could compromise research participant privacy, while
605 summary statistics directly generated from genetic data that will precisely reproduce published
606 results are all deposited in Dryad (https://doi.org/10.5061/dryad.4f4qrfjd0). Custom scripts for
607 generating summary statistics and all results are deposited in GitHub
608 (https://github.com/Chuxj/Gf_of_ip_in_T1D).

609

610 **Ethical statement**

611 The 500FG-DM study was approved by the ethical committee of Radboud University Nijmegen
612 (NL-number: 54214.091.15). Experiments were conducted according to the principles expressed
613 in the Declaration of Helsinki. Written informed consent was obtained from all participants.

614

615 **Figure legends:**

616 **Figure 1**. Overview of data and experimental design. **A**, Schematic study design. **B**,**C**, Cell (**B**)
617 and cytokine (**C**) type relationship visualized by non-metric multidimensional scale
618 (NMDS) analysis in 300DM, where B cell traits (red) are clustered separately from T cell
619 and monocyte traits (B) and cytokines with same cellular origins are clustered together
620 (C) In panel **B**, Small dots indicate the proportion of subpopulations and large dots
621 indicate counts of their parental cell types. Circles represent the calculated centroid of the
622 grouped cell and cytokine types at confidence level 0.95. **D**, Heatmap of correlation
623 coefficients between immune cell counts (y-axis) and cytokine production in response to
624 stimulations (x-axis) in T1D patients. Significant correlations (FDR <0.05) are labeled by
625 dots, with the color indicating correlation coefficients. Positive correlations (red) are
626 observed between monocyte traits and monocyte-derived cytokines (top left), and
627 between adaptive immune cell counts and T cell-derived cytokines (bottom right).
628 Negative correlations (blue) are observed between adaptive immune cell counts and
629 monocyte-derived cytokines.

630

631

632 **Figure 2.** Impact of T1D GWAS SNPs on immune phenotypes. **A**, QQ plots of QTL profiles of
633 62 T1D GWAS loci grouped by cell populations. The distribution of P values of
634 associations with T cells traits (blue) show a significant deviation from an expected
635 uniform distribution (dashed line). **B**, Histogram showing number of associations
636 observed (red line) and those in permutations (blue bars). **C**, Heatmap of QTL profiles of
637 cell proportion carrying certain chemokine receptors across 62 T1D GWAS loci, colored
638 by -log10(p values) and effect direction of T1D risk allele. Arrowhead indicates a T1D
639 risk allele rs11574435-T.

640

641

642 **Figure 3.** Impact of T1D GWAS SNPs on immune phenotypes. **A**, Expression of *CCR5*, *CCL5*
643 and *CCL4* in PBMCs (top) and Pancreases (bottom) altered in T1D patients (blue, green
644 and purple) compared to healthy controls (red). **B**, A locus zoom plot showing SNPs
645 around rs35092096 located in CCR region are associated with CCR6+CCR7-CCR5+ T
646 reg proportion. **C**, A boxplot showing CCR6+CCR7-CCR5+ T reg proportion differs in
647 different rs35092096 genotypes (TT: red, TG: green and GG: blue). **D**, Two locus zoom
648 plots indicating colocalization between CCR6+CCR7-CCR5+ T reg proportion QTL
649 profiles (top, red) and T1D GWAS profile (bottom, blue) within CCR regions.

650

651 **Figure 4.** Genetic regulators on immune phenotypes. **A**, Three Manhattan plots showing genetic
652 regulators of immune cell proportion (top), proportion of immune cells expressing CCR
653 (middle) and cytokines production in response to stimulations (bottom). P values of SNPs

654 identified in meta-analysis were colored in red. **B**, A locus zoom plot showing a T1D
655 specific regulatory locus around rs4744112 that effects CCR6+CXCR3+CCR4- T
656 helper1 proportion. **C**, A boxplot showing CCR6+CXCR3+CCR4- T helper1 proportion
657 varies in different rs4744112 genotypes (TT: red, TG: green and GG: blue).

658

659

660

661

662

663 **Figure supplement legends:**

664 **Figure 1--figure supplement 1.** Heterozygosity check.

665 Left-side panel, an overview of missingness vs heterozygosity for all samples represented by
666 circle; x-axis: Proportion of missing genotypes, y-axis: Heterozygosity rate) and ancestry
667 clustering. Right-side panel, multiple dimensional scaling plot for our T1D samples (red dots) in
668 comparison with reference samples from 1000G. X and y axis correspond to component 1 and
669 component 2 in multiple dimensional scaling plot, respectively. In total, six outliers (red symbols
670 from either left or right panel) were removed in further analysis.

671 **Figure 1 - Figure supplement 2.** Flow cytometry gating strategy of the chemokine receptor
672 panel.

673 **Figure1 - Figure supplement 3.** Correlation between cell counts and cytokine production in
674 healthy individuals.

675 Heatmap of correlation coefficients (indicated by colors) between immune cell counts (y-axis)

676 and cytokine production in response to stimulations (x-axis) in healthy individuals (500FG),
677 which is consistent with 300DM.
678
679 **Figure 2 - Figure supplement 1.** QQplots of QTL profiles of 62 T1D GWAS loci grouped by
680 cytokine types.
681 **Figure 2 - Figure supplement 2.** Impact of T1D GWAS SNPs on immune phenotypes.
682 **A**,**B**, Heatmap of QTL profiles of immune phenotypes across 62 T1D GWAS loci, colored by -
683 log10(p values) and effect direction of T1D risk allele (**A**: immune cell proportion traits; **B**:
684 cytokine production upon stimulations).
685
686 **Figure 4 -- Figure supplement 1**. Enriched pathways of QTLs found for immune phenotypes.
687 Pathway enrichment analysis using genes located within immune cell proportion QTLs (**A**) and
688 cytokine production QTLs (**B**).
689 **Figure 4—figure supplement 2**. Functional annotation of the immune phenotypes associated
690 SNPs ($P < 5\times10^{-8}$).
691 Stacked boxplots showing the percentage of genomic elements where the immune phenotypes
692 associated SNPs located.
693 **Figure 4—figure supplement 3.** Impact of age, gender and seasons on immune phenotypes.
694 **A, B**, Heatmaps of correlation between immune cell counts (y-axis) and age, gender, seasons (x-
695 axis). Correlation coefficients were indicated by colors, and significant correlations (FDR <0.05)
696 are labeled by dots. **C**, Heatmap of correlation between cytokines levels upon stimulations and
697 age, gender, seasons. Correlation coefficients were indicated by colors, and significant
698 correlations (FDR <0.05) are labeled by dots.

Fig. 1

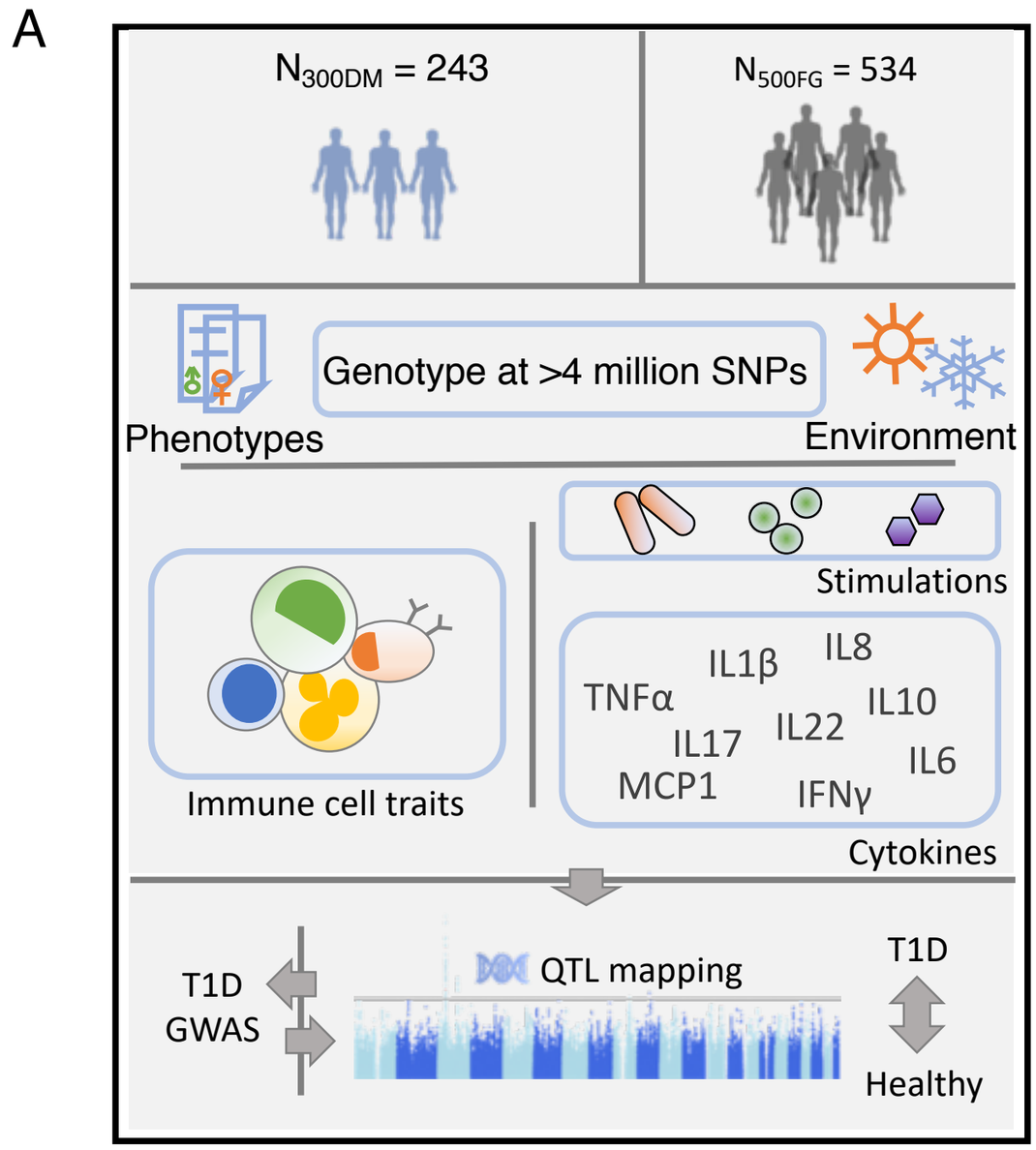
A
N300DM = 243
N500FG = 534
Genotype at >4 million SNPs
Phenotypes
Environment
Stimulations
Immune cell traits
TNFα
IL1β
IL8
IL10
IL17
IL22
IL6
MCP1
IFNγ
Cytokines
T1D GWAS
QTL mapping
T1D
Healthy

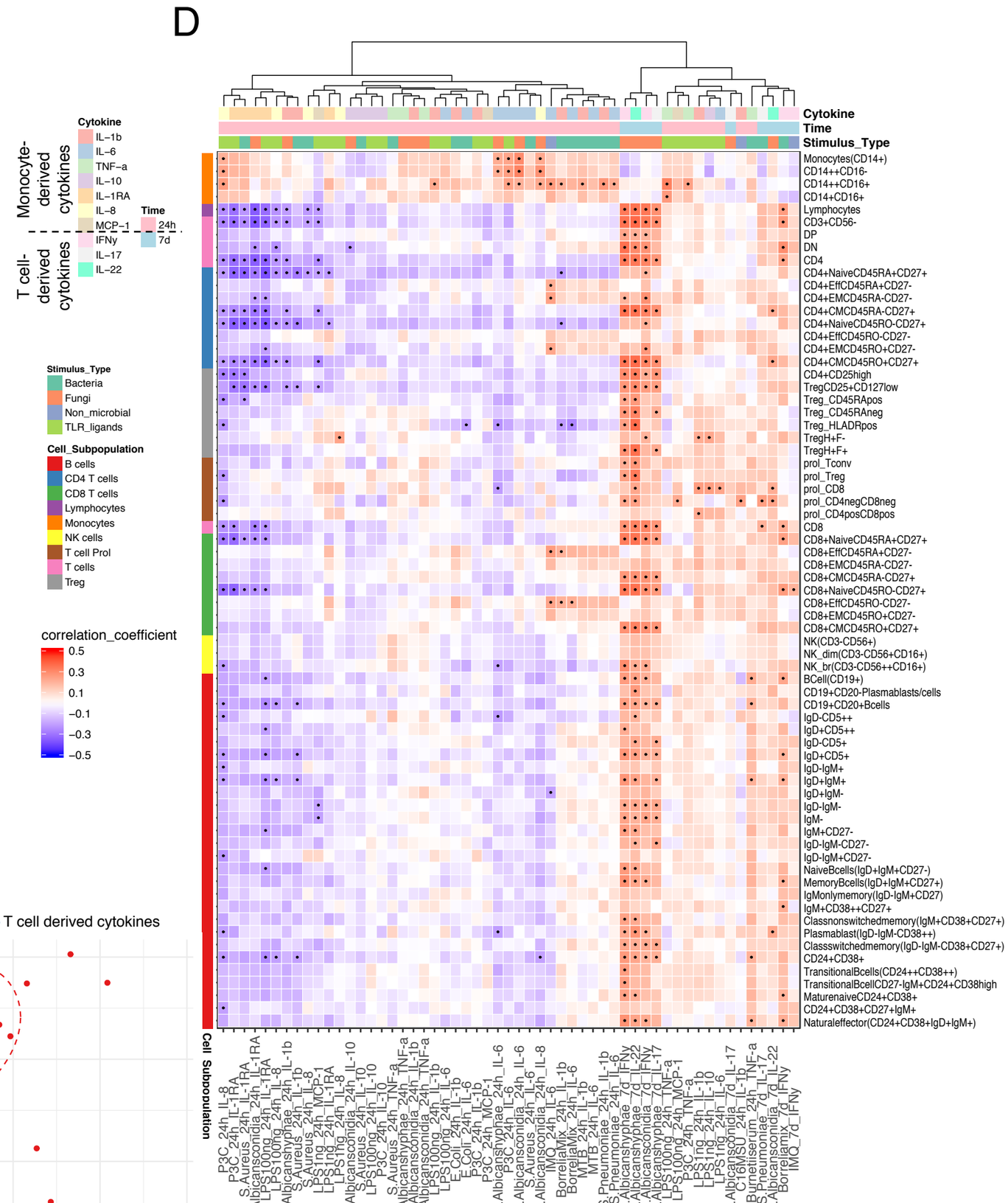
D
Cytokine
Time
Stimulus_Type
Monocyte-derived cytokines
T cell-derived cytokines
IL−1b
IL−6
TNF−a
IL−10
IL−1RA
IL−8
MCP−1
IFNγ
IL−17
IL−22
24h
7d
Stimulus_Type
Bacteria
Fungi
Non_microbial
TLR_ligands
Cell_Subpopulation
B cells
CD4 T cells
CD8 T cells
Lymphocytes
Monocytes
NK cells
T cell Prol
T cells
Treg
correlation_coefficient
0.5
0.3
0.1
−0.1
−0.3
−0.5
Cell Subpopulation

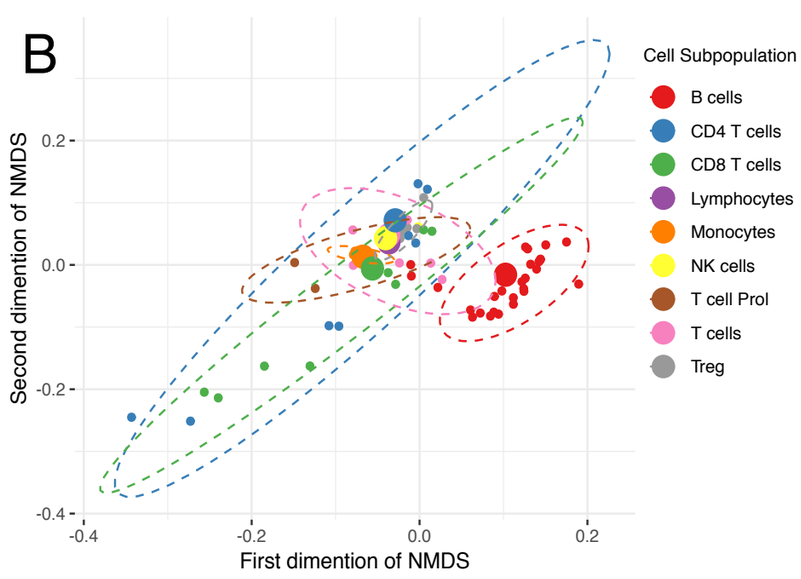
B
Cell Subpopulation
B cells
CD4 T cells
CD8 T cells
Lymphocytes
Monocytes
NK cells
T cell Prol
T cells
Treg
Second dimention of NMDS
First dimention of NMDS

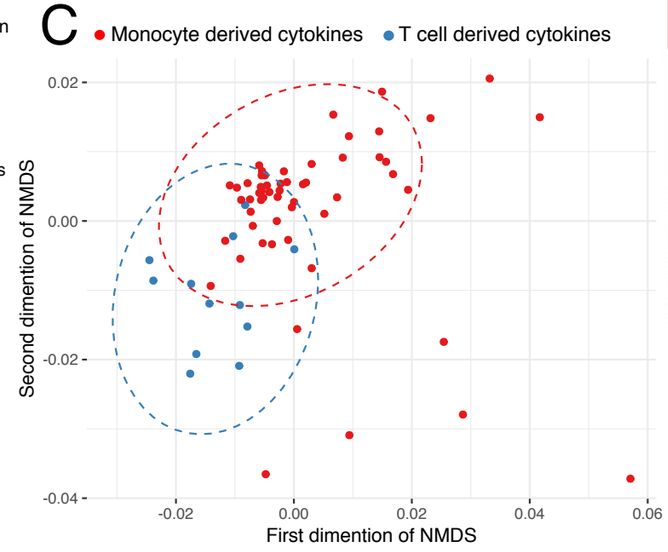
C
Monocyte derived cytokines
T cell derived cytokines
Second dimention of NMDS
First dimention of NMDS

Fig. 2

A

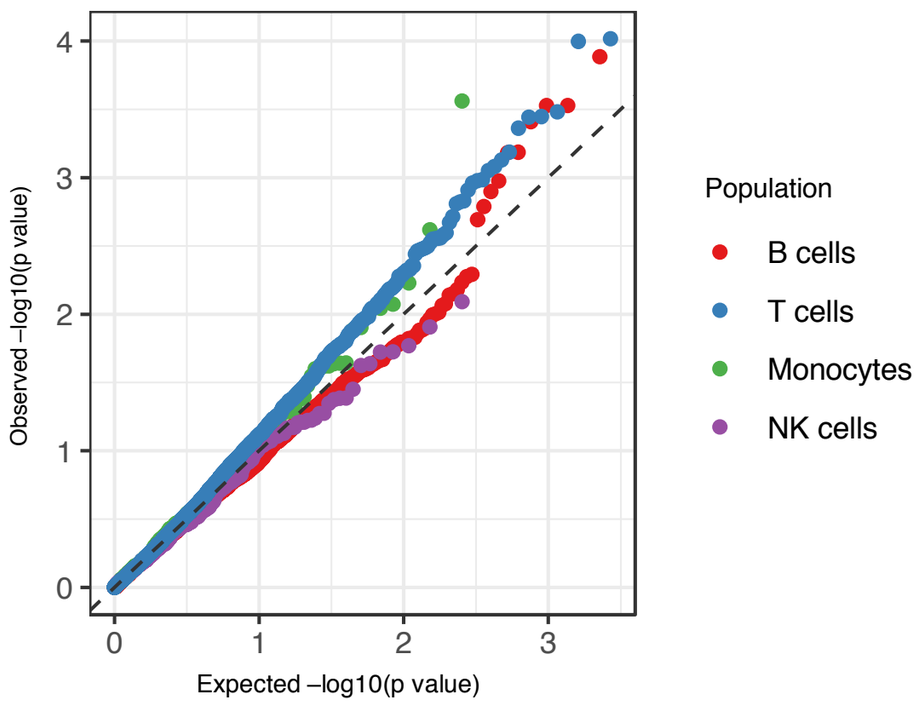
Observed −log10(p value)
Expected −log10(p value)
0
1
2
3
4
Population
B cells
T cells
Monocytes
NK cells

B

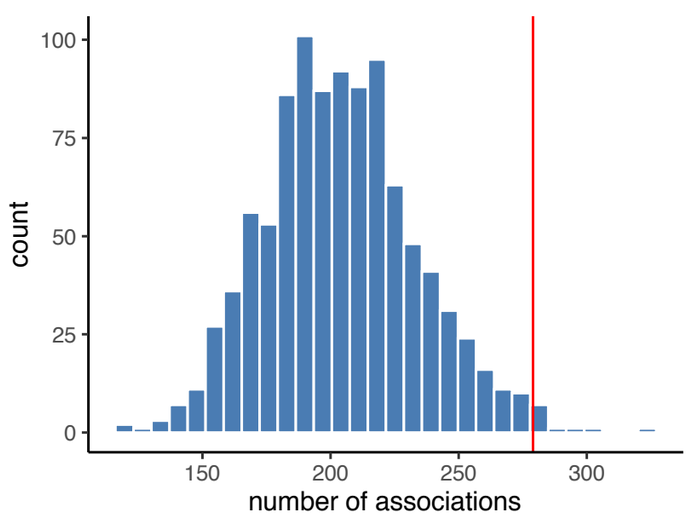
count
number of associations
0
25
50
75
100
150
200
250
300

C

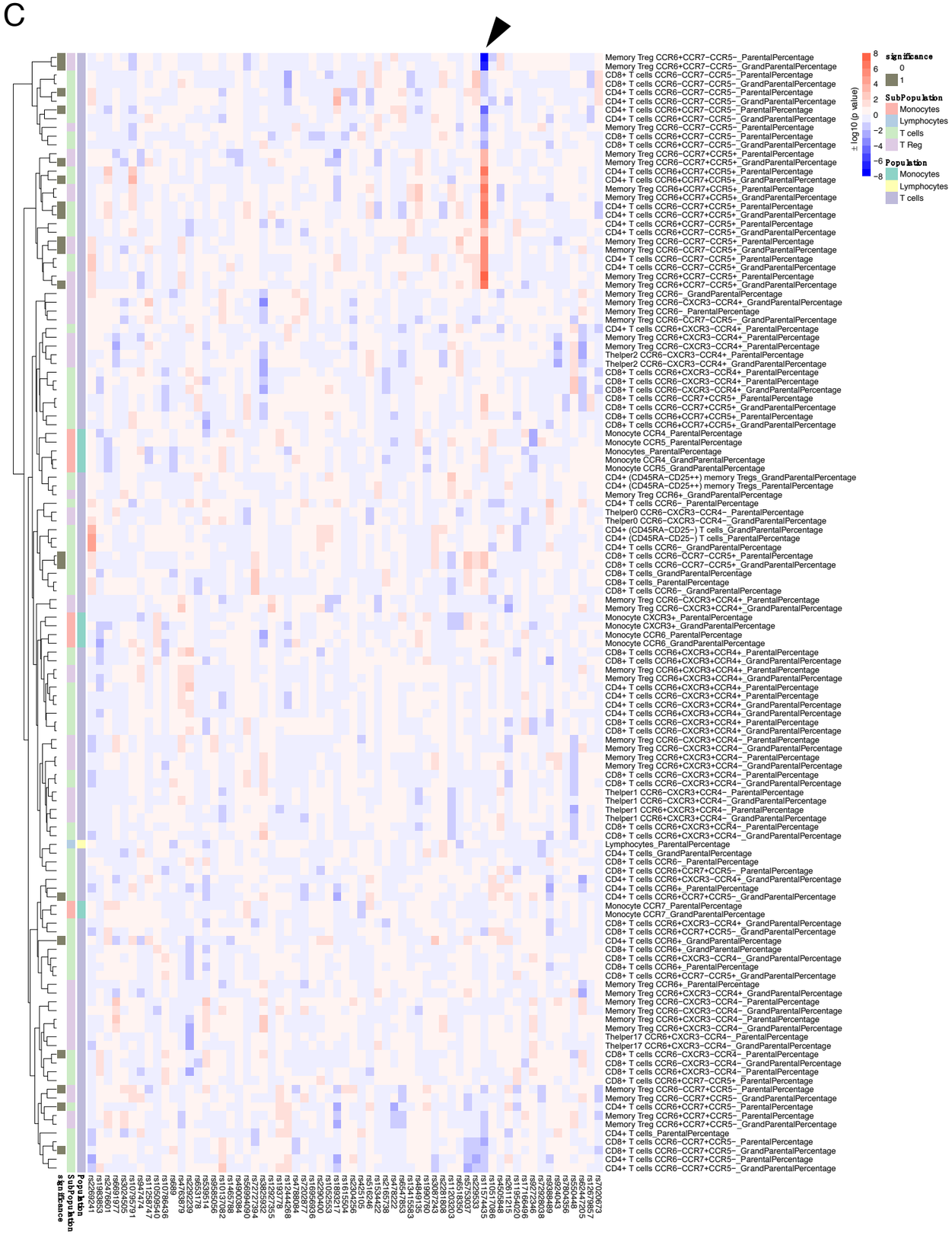
significance
0
1
SubPopulation
Monocytes
Lymphocytes
T cells
T Reg
Population
Monocytes
Lymphocytes
T cells
± log10 (p value)
8
6
4
2
0
−2
−4
−6
−8

Fig. 3

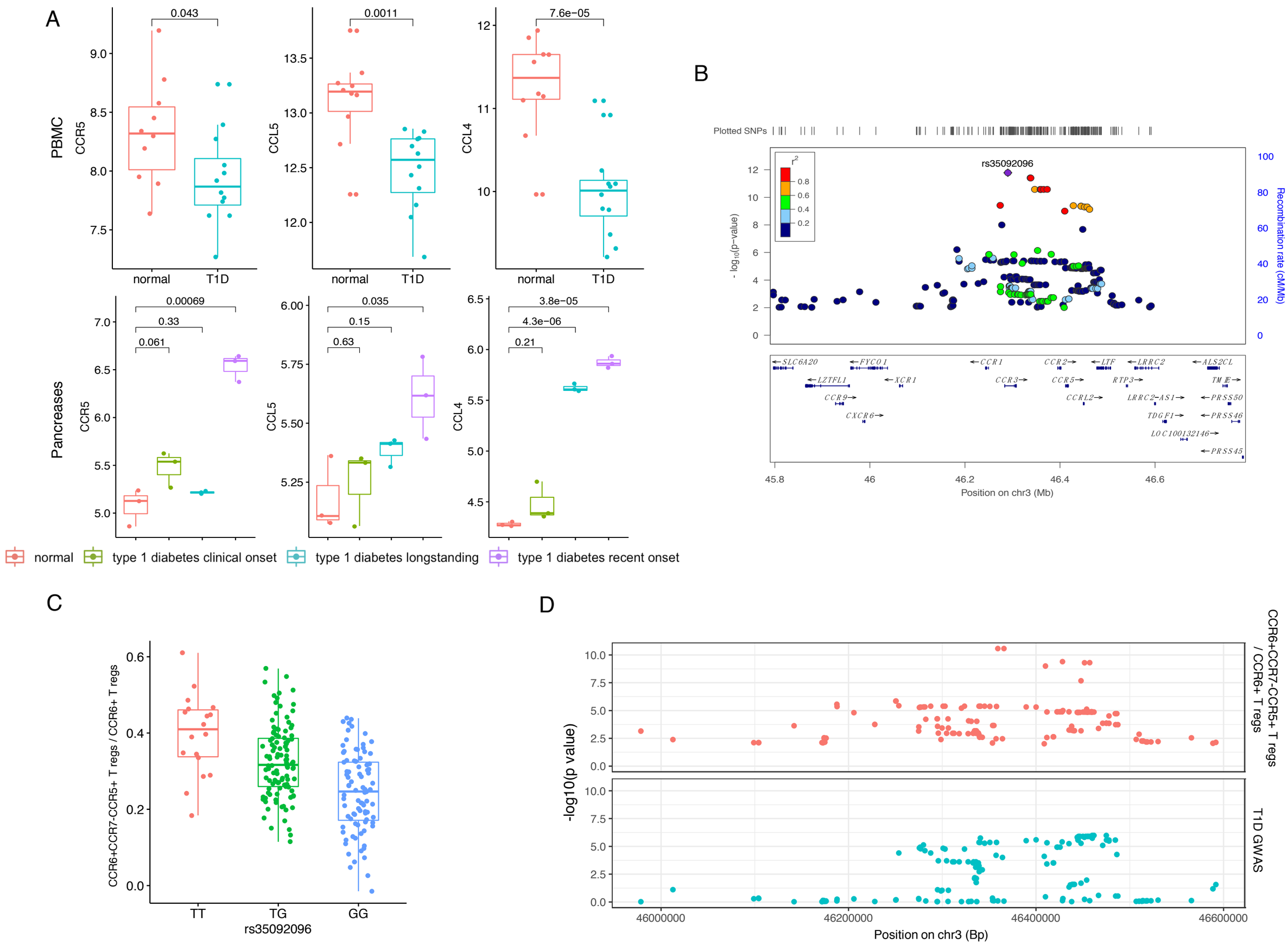
A
PBMC
CCR5
CCL5
CCL4
0.043
0.0011
7.6e−05
normal
T1D
Pancreases
0.00069
0.33
0.061
0.035
0.15
0.63
3.8e−05
4.3e−06
0.21
normal
type 1 diabetes clinical onset
type 1 diabetes longstanding
type 1 diabetes recent onset
B
Plotted SNPs
rs35092096
- log10(p−value)
Recombination rate (cM/Mb)
Position on chr3 (Mb)
SLC6A20
FYCO1
CCR1
CCR2
LTF
LRRC2
ALS2CL
LZTFL1
XCR1
CCR3
CCR5
RTP3
TMEF
CCR9
CCRL2
LRRC2-AS1
PRSS50
CXCR6
TDGF1
PRSS46
LOC100132146
PRSS45
C
CCR6+CCR7-CCR5+ T regs / CCR6+ T regs
TT
TG
GG
rs35092096
D
-log10(p value)
CCR6+CCR7-CCR5+ T regs / CCR6+ T regs
T1D GWAS
Position on chr3 (Bp)

Fig. 4

A

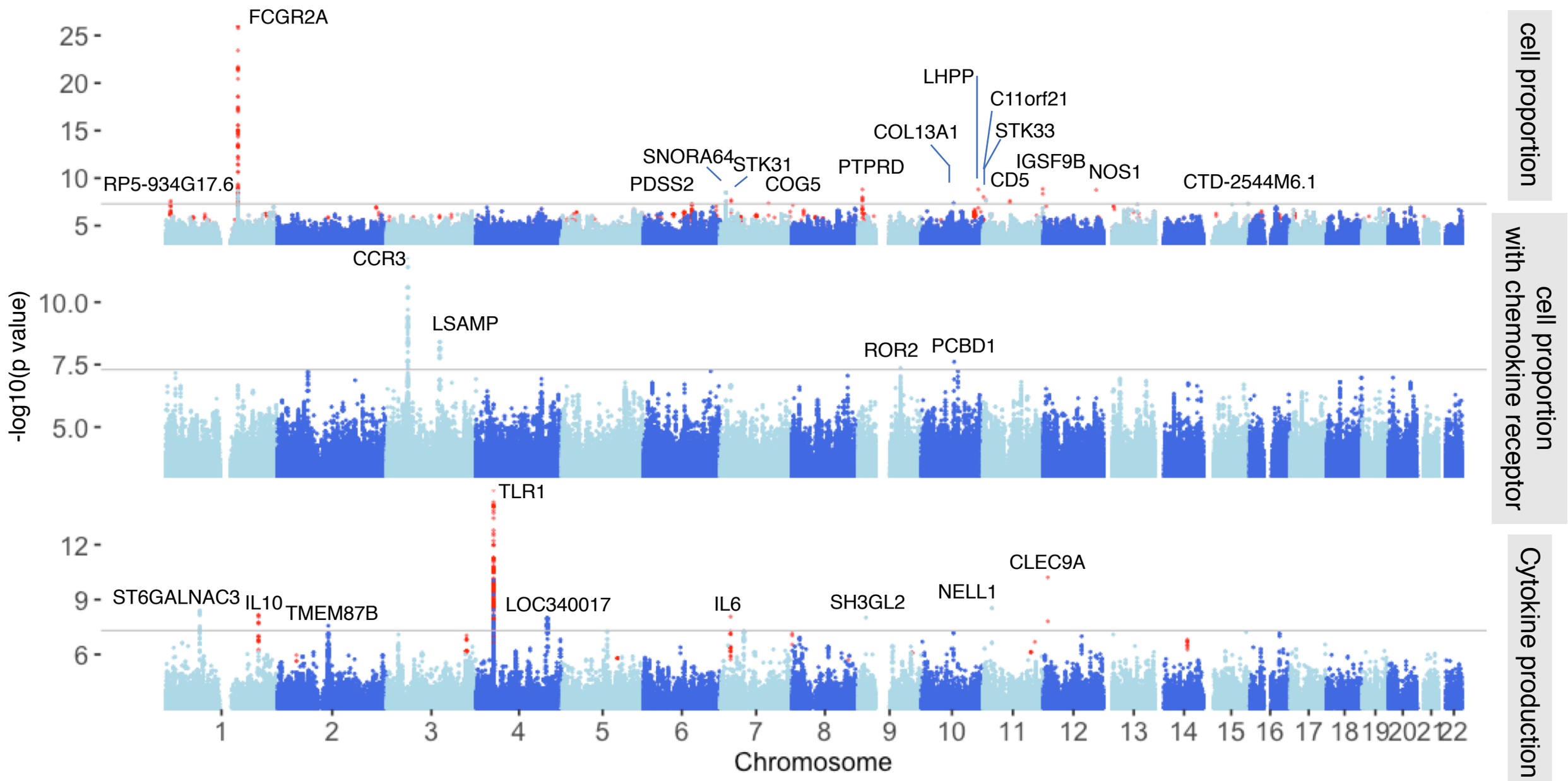
FCGR2A
RP5-934G17.6
CCR3
LSAMP
SNORA64
STK31
PDSS2
COG5
PTPRD
COL13A1
LHPP
C11orf21
STK33
IGSF9B
CD5
NOS1
CTD-2544M6.1
ROR2
PCBD1
TLR1
ST6GALNAC3
IL10
TMEM87B
LOC340017
IL6
SH3GL2
NELL1
CLEC9A
-log10(p value)
Chromosome
cell proportion
cell proportion with chemokine receptor
Cytokine production

B

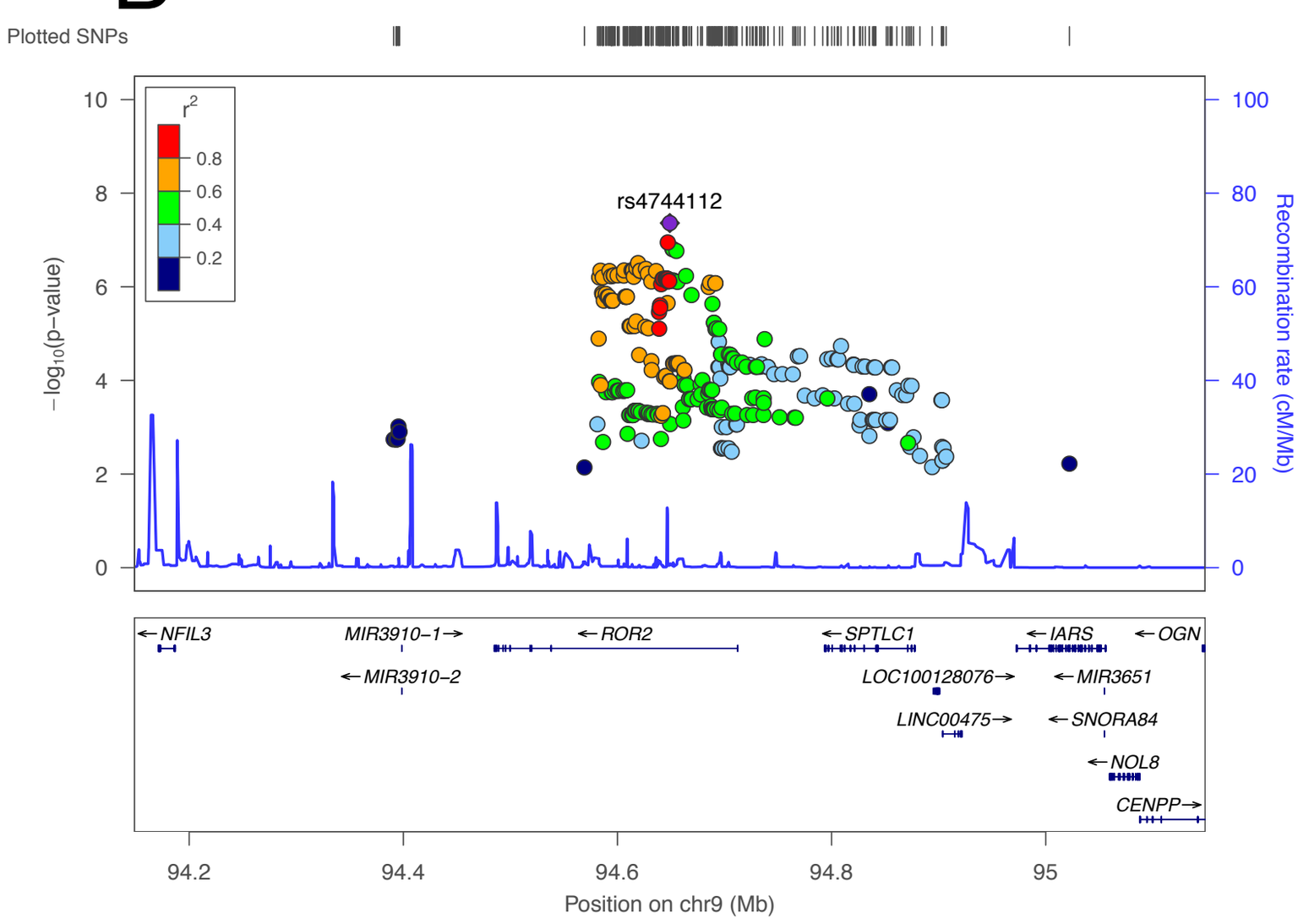
Plotted SNPs
rs4744112
r2
0.8
0.6
0.4
0.2
−log10(p−value)
Recombination rate (cM/Mb)
NFIL3
MIR3910−1
ROR2
SPTLC1
IARS
OGN
MIR3910−2
LOC100128076
MIR3651
LINC00475
SNORA84
NOL8
CENPP
Position on chr9 (Mb)

C

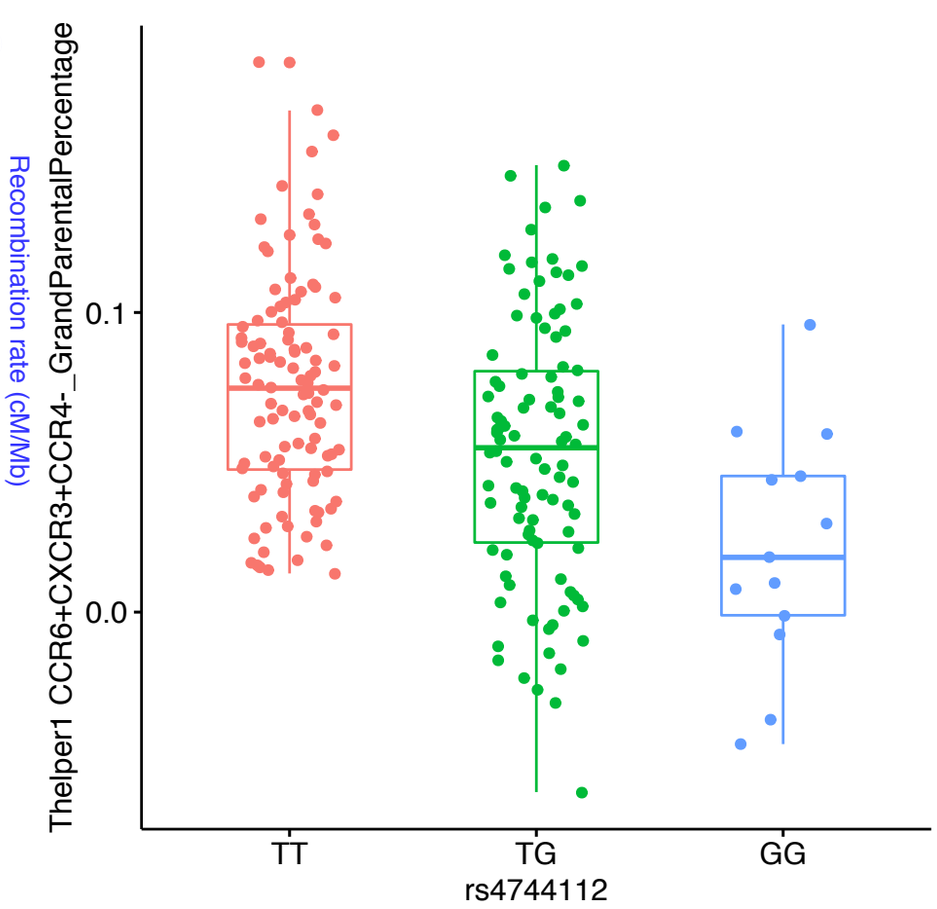
Thelper1 CCR6+CXCR3+CCR4-_GrandParentalPercentage
TT
TG
GG
rs4744112

Figure 1—figure supplement 1.

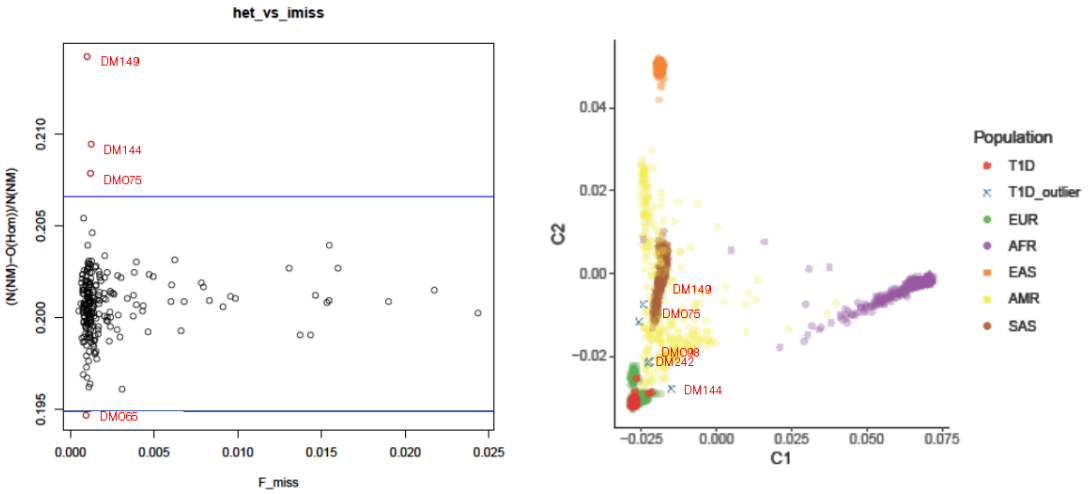

Figure 1—figure supplement 2.

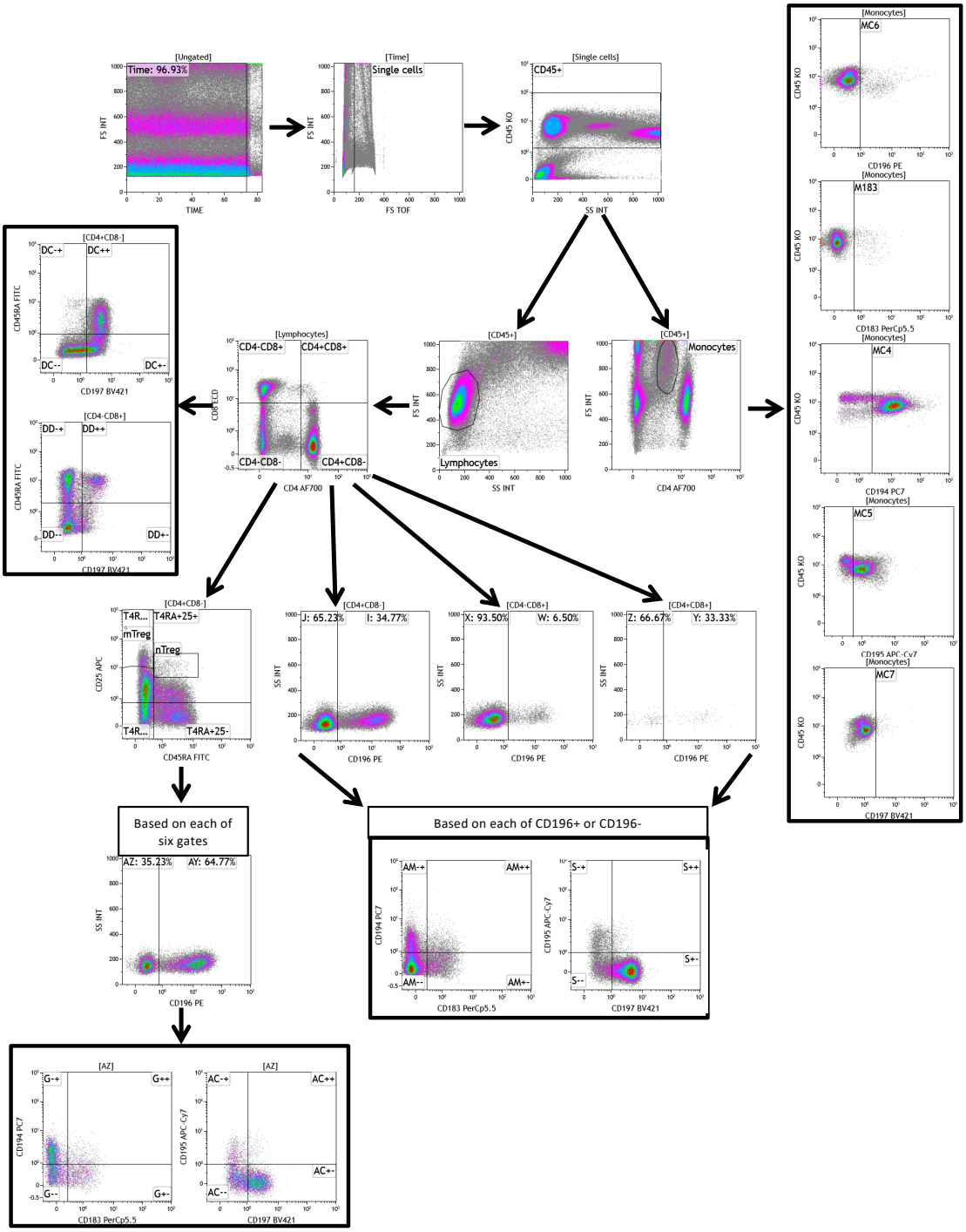

Figure 1—figure supplement 3.

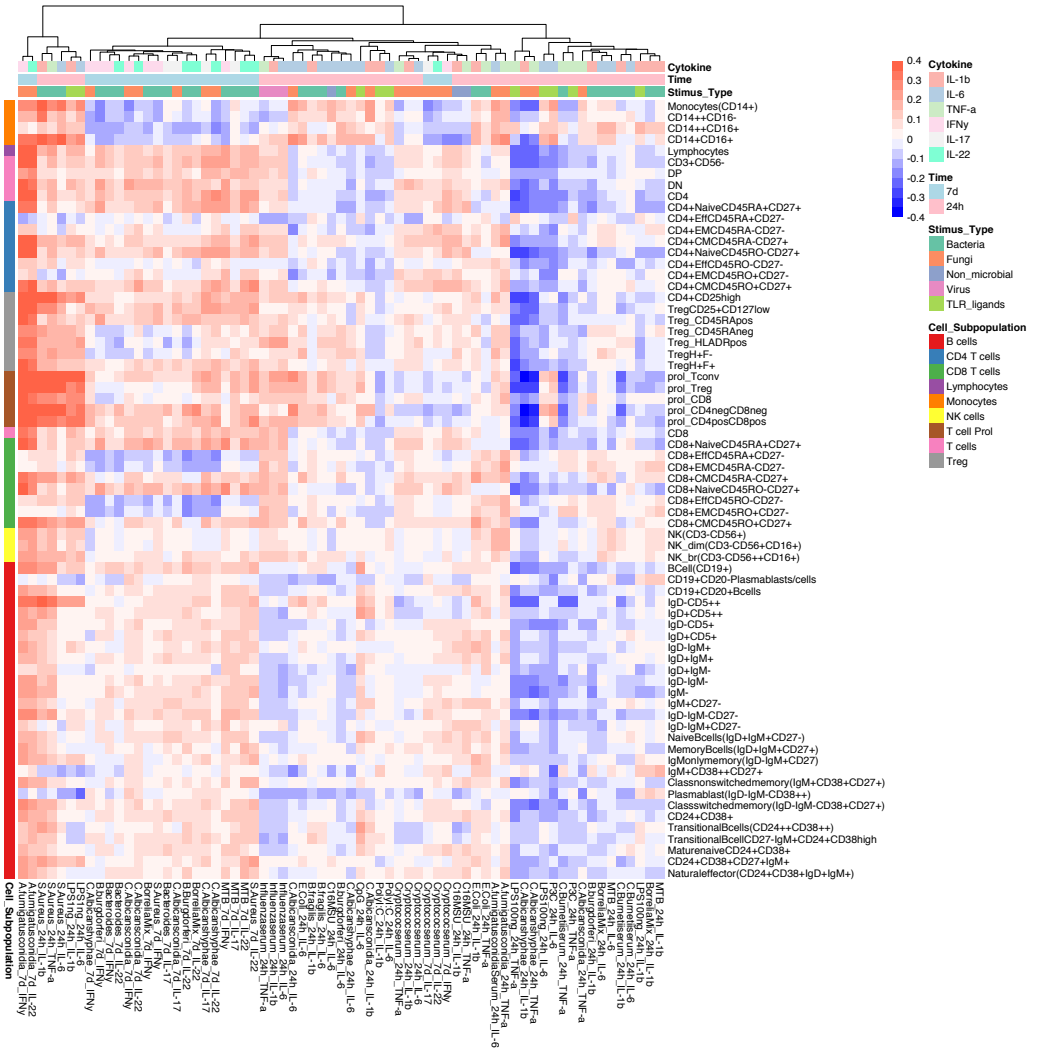

Figure 2—figure supplement 1.

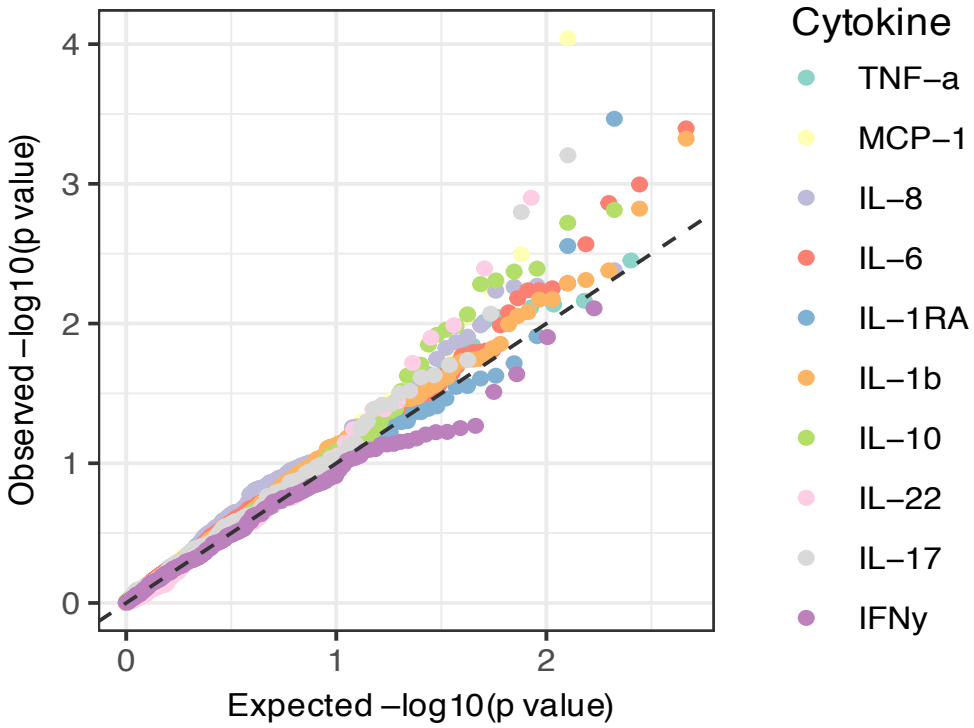

Figure 2—figure supplement 2.

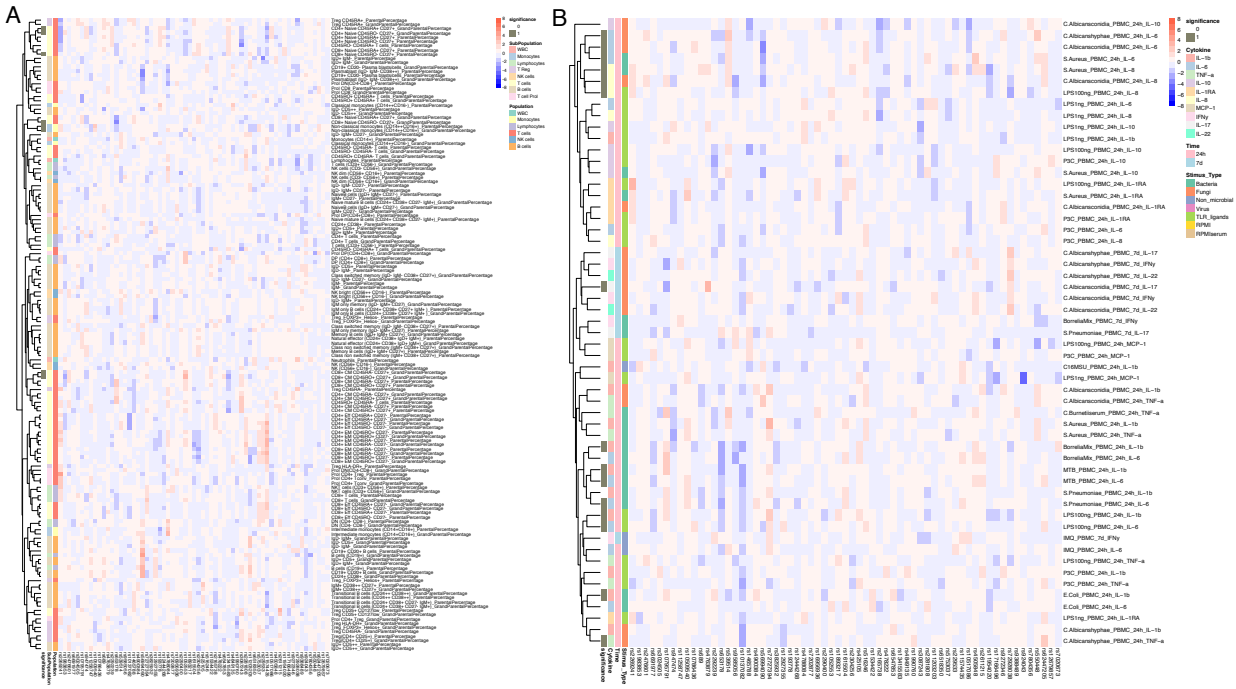

Figure 4—figure supplement 1.

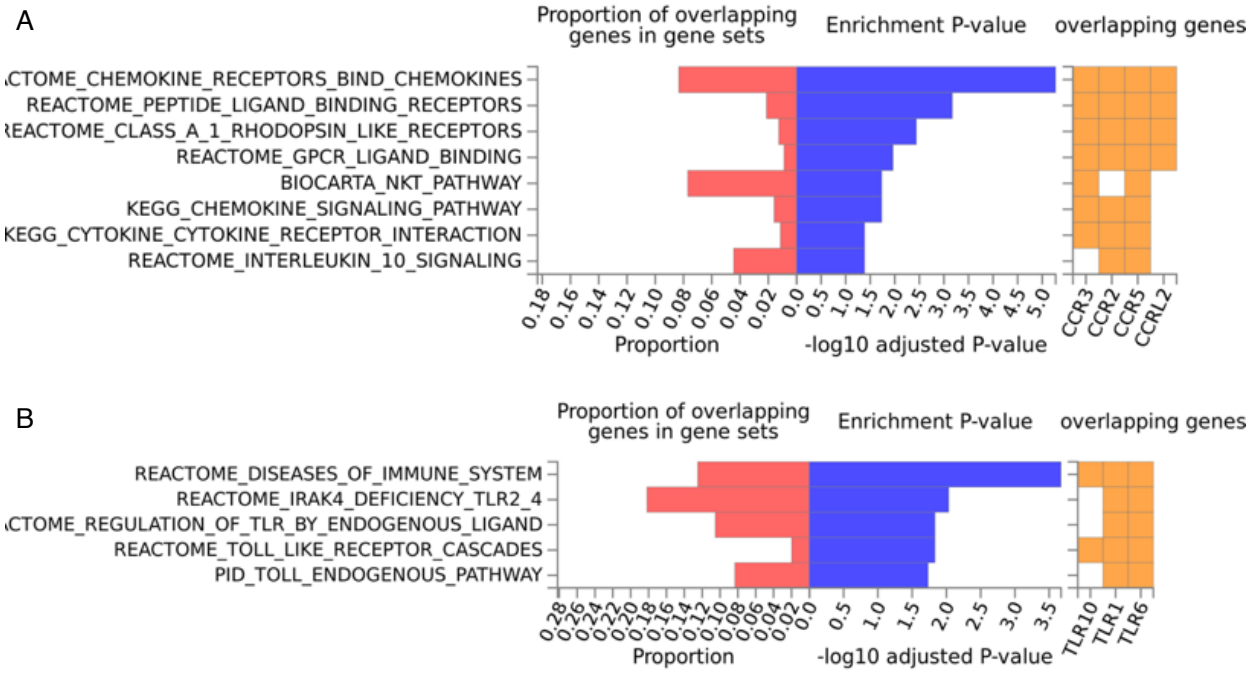

Figure 4—figure supplement 2.

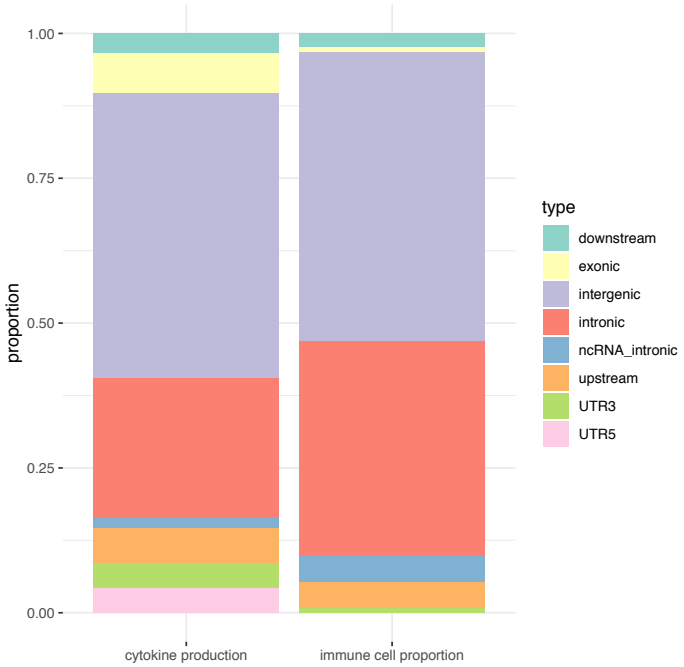
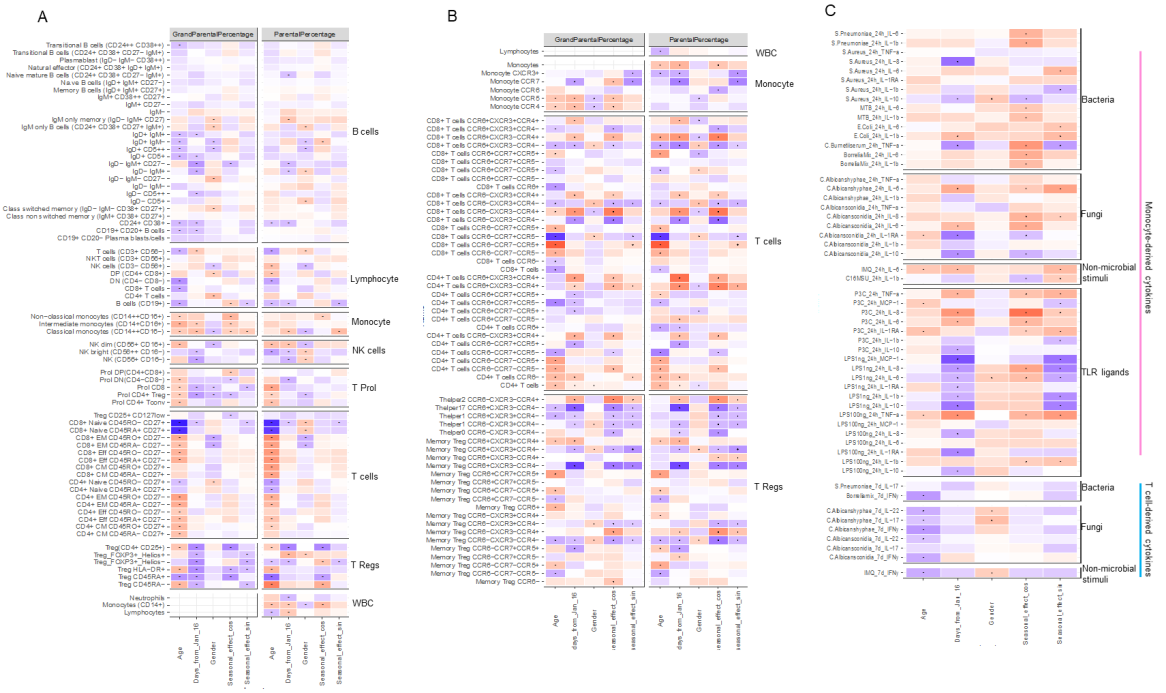
Figure 4—figure supplement 3.